SAPIENZA
UNIVERSITÀ DI ROMA

PhD program in Cellular and Development Biology

Dipt. of Biology and Biotecnology

PhD Thesis

The COP9 signalosome is involved in the regulation of lipid metabolism and of transition metals uptake in Saccharomyces cerevisiae

Chiara Salvi

Supervisor: Dott.ssa Teresa Rinaldi

Tutor: Prof. Rodolfo Negri

XXVI Ciclo - Anno Accademico 2013-2014

TABLE OF CONTENTS

ABSTRACT

The COP9 signalosome (CSN) is a highly conserved eukaryotic protein complex which regulates the Cullin-RING family of ubiquitin ligases and carries out a deneddylase activity that resides in subunit 5 (CSN5). Whereas CSN activity is essential for higher eukaryotes development, several unicellular fungi, including the budding yeast *S. cerevisiae*, can survive without a functional CSN. Nevertheless, the budding yeast CSN is biochemically active and deletion mutants of each of its subunits exhibit deficiency in deneddylation of cullins, although the biological context of this activity is still unknown in this organism. To further characterize CSN function in budding yeast, in this thesis I present a transcriptomic and a proteomic analysis of a *S. cerevisiae* strain deleted in *CSN5*, coding for the only canonical subunit of the complex. We discovered that Csn5 is involved in the modulation of the genes controlling aminoacid and lipid metabolism, and especially ergosterol biosynthesis. These alterations in gene expression correlate with the lower ergosterol levels and increased intracellular zinc content which we observed in *csn5* null mutant cells. We show that some of these regulatory effects of Csn5, in particular the control of isoprenoid biosynthesis, are conserved through evolution, since similar transcriptomic and/or proteomic effects of csn5 mutation were previously observed in other eukaryotic organisms such as *As. nidulans*, *A. thaliana* and *D. melanogaster*. Our results suggest that the diverged budding yeast Csn is more conserved than was previously thought.

INTRODUCTION

1.1 The Cop9 signalosome (CSN)

The Cop9 signalosome (CSN) is a highly conserved eukaryotic complex with a canonical composition of 8-subunit, that was initially discovered as a repressor of light-regulated development in *Arabidopsis thaliana* [1 - 3]. Subsequently, the CSN was found also in other eukaryotes such as *D. melanogaster, S. cerevisiae, S. pombe, C. elegans* [1]. The complex has been shown to regulate diverse cellular processes, ranging from cell-cycle progression and signal transduction to transcription regulation [4 - 8]. Despite the wide spectrum of CSN functions, a common theme has become apparent suggesting that many of these functions are tied to the ubiquitin mediated proteolysis pathway.

A canonical CSN is composed of eight subunits (CSN1-8), 6 subunits (CSN1-4; CSN7-8) harbouring a PCI domain (Proteasome, COP9 and Initiation factor 3), and 2 subunits (CSN5-6) harbouring an MPN domain [9 - 11].

The best-studied function of the CSN is the enzymatic regulation of Cullin RING ubiquitin E3 Ligases (CRLs) in the ubiquitin proteasome system (UPS) [1]. CRLs are heteromeric enzymes comprising cullin, RING domain, and substrate receptor subunits [12]. The cullin subunit serves as the backbone of the enzyme, displaying on one end a substrate receptor complex that recruits substrates for ubiquitylation and on the other end a RING domain subunit (Rbx1/Roc1/Hrt1) that recruits a ubiquitin-conjugating enzyme that transfers ubiquitin to substrate. CSN forms a stable complex with a particular subfamily of CRLs know as SCF ubiquitin ligases [13]. CRLs are active when covalently attached to the ubiquitin-related protein, Nedd8 (known as Rub1 in plants and budding yeast). Neddylation/deneddylation cycles are required for the regulation of CRL function, and the CSN mediates deneddylation. Deneddylation of cullins resides in its subunit CSN5, which catalyzes the deconjugation of the small peptide Nedd8 from the cullin subunit of CRL [4] (Fig. 1).

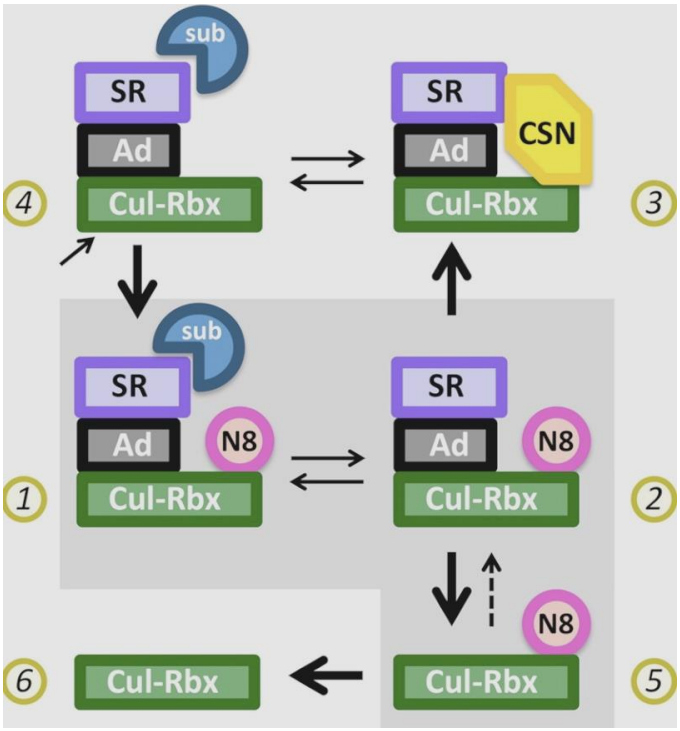

Fig. 1 Regulation of CRLs by reversible neddylation [14].

Accumulation of substrate for a particular CRL complex would be expected to lead to accumulation of the Nedd8-conjugated form of that complex (step 1). Upon consumption of the substrate (step 2), the CRL complex would either be subject to autoubiquitylation and degradation of the substrate receptor (step 5) or recruit CSN and be deneddylated (step 3). Reappearance of substrate would lead to displacement of CSN (step 4) and re-formation of neddylated, active complex (step 1). By this mechanism, CRL complexes for which substrate is present would be preferentially neddylated and activated. In the absence of CSN (gray zone), this regulation would be undermined, and upon depletion of substrate for a particular CRL, the complex would remain conjugated to Nedd8 and active (step 2), leading to autoubiquitylation and ultimately degradation of the substrate receptor and inactivation of the CRL (step 5).

Cul (Cullin); Rbx (Ring domain subunit); Ad (Adaptor subunit); SR (Recognition substrate subunit); Sub (Substrate) and N8 (Nedd8).

CSN5, is a highly conserved subunit that harbors a unique catalytically active metal binding MPN+/JAMM metalloprotease motif responsible for isopeptidase activity that is dependent on integrated CSN complex [15 - 16]. The opposite event -conjugation of Nedd8 to cullins- stimulates CRL activity [17 - 20]. The observed positive role of CSN in regulating CRL activity can be explained by the finding that CSN-mediated inactivation of CRLs counteracts autocatalytic breakdown of CRL substrate receptor subunits [21 - 23]. Recent data suggest, however, that CSN regulation of CRLs can also occur in non-enzymatic fashion, suggesting that CSN regulates CRL activity by multiple mechanisms [14, 24 - 26].

Interestingly, the MPN+/JAMM domain exists in pairs with a MPN- (a MPN domain that lacks the JAMM catalytic motif) subunit such as CSN6. Little is know about whether the MPN- domain contributes to the enzymatic activity of the complex although there have been speculation that the MPN- domain might have a role in the JAMM-dependent activity [27]. Currently it has been speculated that CSN6 MPN- domain plays a role in the structural integrity of the complex [28-29]. The CSN belongs to a family of protein complexes known as the PCI complexes which include also the lid subcomplexes of the 26S proteasome and the eukaryotic translation initiation factor-3 (eIF3) [30]. Members of this family play key roles in the regulation of protein life span from translation to degradation [30 - 32]. Subunit of these complexes share large structural elements such as PCI or MPN domains and are arranged in a comparable architecture [33]. The PCI domain, which is found in six subunits of each complex, serves as a structural scaffold that supports complex integrity via interactions between subunits [33 - 35]. This has been also revealed by the crystallographic data of the PCI domain of *Arabidopsis thaliana* subunit 7 [28]. Biochemical size fractionation analysis indicates that few CSN subunits are monomeric or in smaller versions of the CSN ("mini-CSN") (Fig. 2).

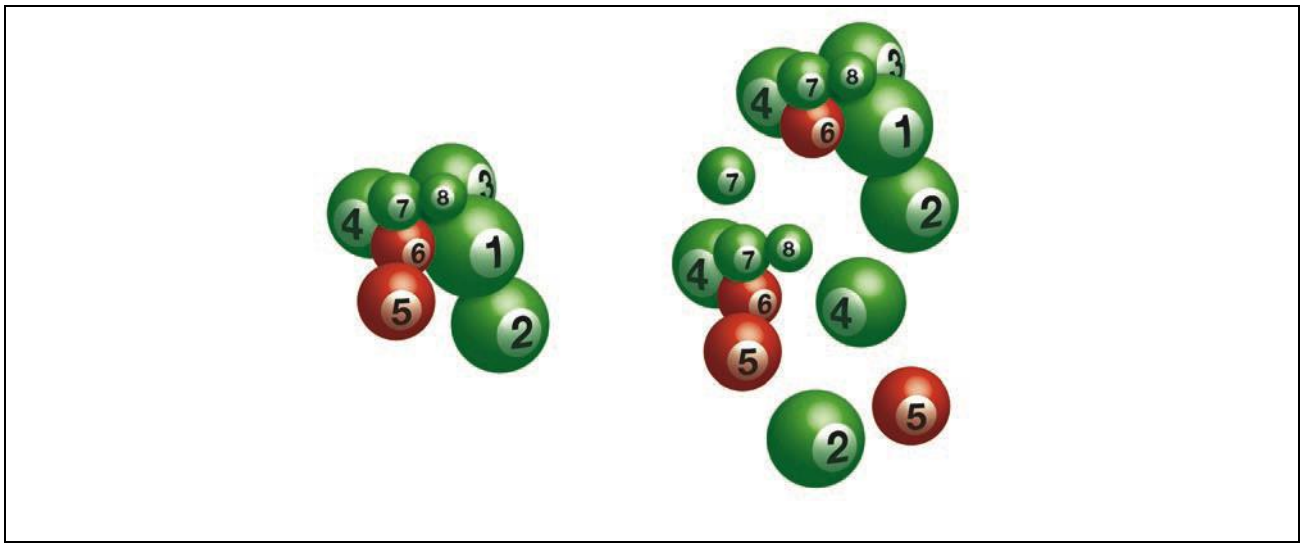

Fig. 2 Comparison between the eight-subunit CSN and 'mini CSN' [36].

The size of each ball is proportional to the protein size. The green balls represent PCI-domain subunits and the red balls represent MPN-domain subunits. The subunit architecture is shown according to [29].

Interestingly, CSN5 is a common components of many of the small CSN complexes [37] and a large fraction of overexpressed CSN5 is found in a free form [38]. Although the CSN-associated CSN5 is mostly nuclear, the free form of CSN5 appears to be both cytoplasmic and nuclear [39], and latter might reflect a nuclear export activity for CSN5. Whether individual CSN subunits, or the minimal CSNs, have indipendent activities, explaining the diverse functionality of the CSN complex, is unclear. Despite the increasing list of biochemical functions assigned to the CSN, to date there are few information regarding the structural arrangements of individual subunits. Recently, the crystal structures of the CSN6 MPN- domain and the hCSN5 subunit have been revealed [40 - 41]. Sharon M. and co-workers [29] reconstituted, coupling the MS and tandem MS results, an interaction network for the eight-component human CSN complex. In this scenario, the complex is composed of two modules, CSN1/2/3/8 and CSN4/5/6/7 connected by interactions between CSN1 and CSN6. Within each module, three of the subunits (CSN1/3/8 and CSN4/6/7) form compact trimers, both binding to additional subunits CSN2 and CSN5 respectively (Fig. 3).

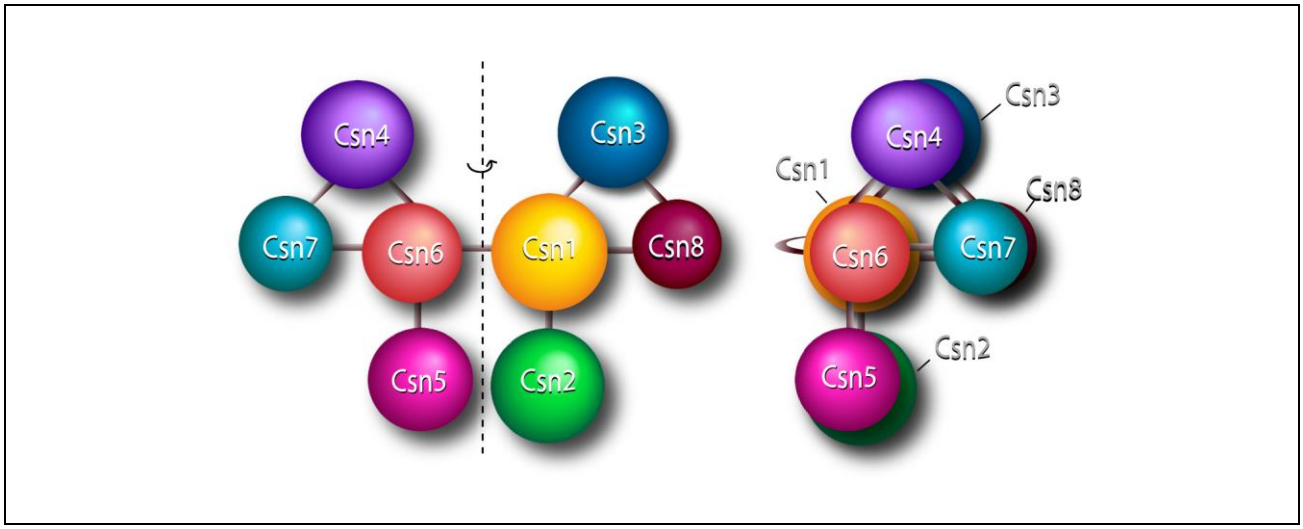

Fig. 3 Modular structure of CSN [29]. See the text for details.

Numerous pair wise interactions were reported for the CSN from fungi, *Arabidopsis*, *Drosophila*, fission yeast, and humans using the yeast two-hybrid system and filter binding assay [39, 42]. These results highlight the essential role of the subunits CSN1 and CSN6 which provide the stable interactions that link the two proteins modules. Interestingly, within each two modules the two peripheral subunits, CSN2 and CSN5, are the most conserved, with over 60% identity between animal and plants [39]. These subunits form extensive interactions with associated proteins in accord with their exposed positions [39, 43].

The modular composition of the Cop9 signalosome can also explain the fact that some subunits of the complex are apparently missing in lower eukaryotic organisms. For example, in *Candida Albicans*, *Cyanidioschyzon merolae* and *Saccharomyces cerevisiae* only four PCI proteins (Csn1, Csn2, Csn3 and Csn7 or their derivatives) plus one MPN+/JAMM protein (Csn5) have been identified [30, 43]. However, these five subunits are sufficient to occupy all specific positions within the module, and it is reasonable to speculate that three of the subunits appear twice in the intact complex.

1.2 The versatile role of CSN5 and of CSN complex

Among the eight CSN subunits, CSN5 can also stably exist independently of the CSN *in vivo* [38]. Several recent studies have explicitly addressed this issue [21, 44 - 47] suggesting the possibility that CSN5 within CSN complex acts as deneddilase but upon release from CSN, would acquire new functions. CSN5, more than any other CSN subunit, can bind numerous cellular regulators exercising different effects on their stability [38, 48]. Two cellular functions are more linked to CSN5 than other CSN subunits: apoptosis and cell proliferation. Csn5 knockout mice exhibit massive apoptosis [49 - 50]; in Csn5-deleted thymocytes there is an increase of expression of the pro-apoptotic protein BCL2-associated X protein (Bax) and decreased expression of anti-apoptotic B-cell CLL lymphoma 2 (Bcl-2) family proteins, including Bcl-xL [49]. Moreover, CSN5 specifically interacts with transcription factor E2F1 and enhances E2F1-dependent apoptosis by a mechanism that is independent of deneddylation activity [47]. Csn5 is involved with the cell proliferation because Csn5 amplification is associated with malignant transformation and many types of human tumors (e.g. breast, pancreatic, prostate, ovarian, certain lung cancers, lymphoma, oral squamous cell carcinomas, hepatocellular carcinoma and melanomas) [46, 48].

As mentioned before the CSN5-deneddylation is only a part of total CSN function. The physiological importance of CSN deneddylation activity in development and cell differentiation was examined in *Drosophila melanogaster*, in which the lethality of *csn-5Δ/Δ* animals was rescued by expression of a CSN-5 transgene but no adult flies were recovered upon equivalent expression of CSN-5 (D148N) (loss of deneddylation activity) [4, 51].

In CSN-5-downregulated HeLa cells, however, the accelerated degradation of c-Jun was rescued equally by over-expression of either the JAMM domain mutant CSN-5D151N or wild-type CSN-5 [52]. These results suggest that the requirement for neddylation/deneddylation cycle of cullins is not absolutely necessary during normal growth and certain developmental stages. In plants, genetic studies suggest that although neddylation/deneddylation cycle is not absolutely necessary during

early embryonic development and germination, it is required during seedling establishment and the later developmental stages [53 - 54].

In *Aspergillus nidulans*, deletion of *csnE/csn-5* or mutation in JAMM domain results in a block in fruiting body formation at the primordial stage, with a few other observed phenotypic changes, such as light-dependent signaling [55 - 56]. Although deneddylation is a major activity of the CSN, it alone cannot explain all of the phenomena described above. These observations raise the possibility that the CSN may have other functional activities in addition to its deneddylation activity. Indeed, if CSN5-mediated deneddylation was the only activity of the CSN, we would expect that loss of CSN5 function would equal loss of the entire complex. In *Drosophila* loss of the entire complex in *csn4* null mutants is much more severe, in terms of transcriptome changes, than the loss of only CSN5 in *csn5* null mutants, which maintain a complex without CSN5 [57]. A similar scenario is described in *S. pombe* in which only *csn1-d* and *csn2-d* mutants and not *csn5-d* mutants- have obvious phenotypes [58]. Also in *A. thaliana* the *csn1* and *csn5* partial-loss of function mutants show different growth phenotypes respect of the null mutants of each subunits that share a common phenotype [59 - 60].

In summary, although CSN5-mediated deneddylation is clearly CSN-dependent function and is essential in most organisms; also the loss of the other subunits of the complex can have different consequences than the loss of only CSN5.

As mentioned before, defects in CSN result in embryonic lethality, presumably because CSN affects various processes at the cellular level including the ubiquitin–proteasome pathway, DNA damage response, cell cycle control and gene expression [1] and also autophagosome maturation as described recently [61 - 63].

1.3 The Cop9 signalosome as a regulator of transcription

Gene transcription and ubiquitin-mediated proteolysis are two processes that have seemingly nothing in common because represent two aspects of life span: the gene expression and the protein degradation. However, many scientific evidences support a key role of the ubiquitin-proteasome system and in particular of the proteasome on the gene expression [64 - 66]. Starting with the discover of the first *csn* mutant, the *A. thaliana csn8* mutant, aberrant expression of light responsive genes has been showed [67]. The CSN was then described as a transcriptional repressor of a range of *Arabidopsis* genes that are normally repressed in the dark. This repression was subsequently correlated to the role of the CSN in controlling the stability of the transcription factors that are stabilized in csn mutants [1, 68]. In addition to light-induced genes, others genes are misregulated in *Arabidopsis* csn mutants such as auxin and jasmonate regulated genes [69 - 70] and genes involved in cell cycle regulation [71].

Studies on mutations of the CSN complex across different organisms have enlighten that the aberrant gene expression is a common phenotype. The mutation of different CSN subunits in *Drosophila* leads to a misregulation of approximately 20% of the transcriptome during larval development [57]. In fact the mutation of *csn* subunits in *Drosophila* leads to severe phenotypes that correlate with transcriptome changes as an indirect consequence. The most obvious among these changes is the achronic expression of numerous developmentally regulated genes [57], the transcription of many of which is usually limited to embryogenesis or metamorphosis. These results indicate that, in the absence of the CSN, the transcription of these genes is derepressed, similar to the derepression of light-activated genes in dark-grown mutants of the *Arabidopsis* CSN.

The CSN plays a role also as a transcriptional activator. As showed in mice, during T-cell development, CSN5 is required for T-cell receptor-driven signals that are involved in positive selection [50] and the specific deletion of Csn8 in T cells leads to an impairment of signal-induced

expression of cell cycle-related genes [72]. For example, in the absence of CSN8, the genes encoding cyclin E1, cyclin D2 and E2f1 are elevated relative to wild-type mice, consistent with the repressive role of the CSN. However, on stimulation for cell-cycle re-entry, the expression of these genes could not be upregulated to wild-type levels.

Braus G.H. and co-workers showed that also in *As. nidulans* the absence of *csn5/csnE* affects transcription of at least 15% of genes during development, including oxidoreductase [73]. In this case the CSN is required for protection against oxidative stress and hormone regulation and for control of the secondary metabolism and cell wall structure [73]. These evidences confirm that the CSN has a role in gene expression but the mechanism/s of this regulation is still unknown. It is less clear if the CSN action is limited to the control of transcription factors stability or if the complex or some subunits can localize to chromatin, suggesting a direct role in transcriptional regulation. To date, there are some indications that suggest a chromatin-associated CSN. In HeLa cells, the CSN is bound to chromatin complexes with the CSA and DDB2-containing E3 ligase complexes during the DNA repair [74]. Ullah and colleagues showed that CSN4 associates with Rbf-target promoters (Retinoblastoma promoters) in *Drosophila* [75]. In these cases, the CSN is supposed to be involved in the stability of transcription factors, but there are evidences that suggest a direct role of the complex on the chromatin. As described in [72] the CSN controls directly the transcription of cell-cycle related genes and in particular they detected by ChIP analysis the Csn1 and Csn8 bound to Cyclin D2, CDK4 and Cdkn1a (encoding p21) promoters. The last evidence supports the idea that some subunits, and maybe the entire complex have the ability to directly control the transcription.

21 years following the initial description of Cop9 signalosome as transcription repressor [67], the mechanisms by which the CSN regulates transcription are being revealed. However much more remains unclear such as the CSN targets, in which form CSN is involved in this regulation and what determines the CSN specificity in transcriptional control.

1.4 The Cop9 signalosome in *Saccharomyces cerevisiae* (*Sc*CSN)

Functional CSN complexes exist in single-cell eukaryotes including protozoa, molds, fungi, and yeasts [42 - 44, 55]. Whereas CSN-encoding genes are strictly essential in metazoans [1] loss of subunit CSN mutants in many unicellular eukaryotes are viable, displaying phenotypes in circadian clock, cell-cycle, pheromone response, and fruit body formation [43, 55, 76 - 78]. Moreover, in several of these species, fewer CSN subunits have been identified [30] (Fig. 4).

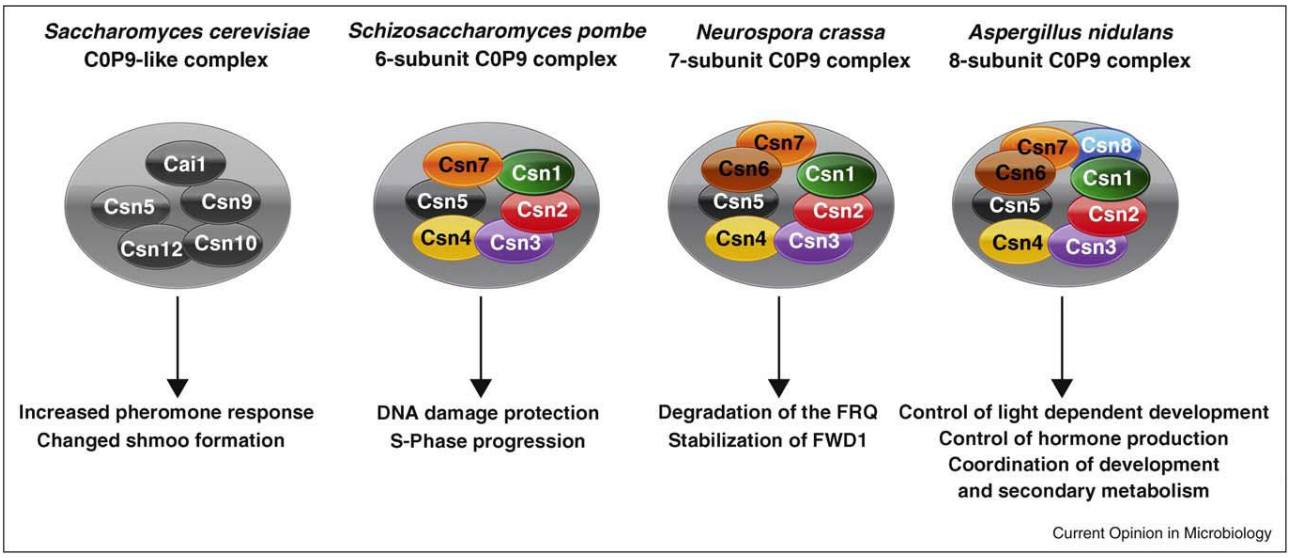

Fig. 4 Overwiev of architecture and developmental functions of fungal COP9 signalosomes [79]

While CSN-deneddylating activity is highly conserved, the budding yeast *Saccharomyces cerevisiae* contains the most divergent CSN-like complex [80]. This suggests that the canonical composition of the CSN complex, comprised of six PCI subunits and a pair of MPN+/MPN- subunits, is not at all a prerequisite for its deneddylase function. In fact, the budding yeast complex, which has, to date, the most simplified subunit composition, represents the minimal CSN 'core' complex sufficient for the enzymatic activity.

The Csn5 is the most conserved subunit and the only canonical subunit within the budding yeast CSN complex [81], and it has been maintained throughout evolution probably because of its essential role in de-neddylation [1, 13, 15, 82 - 83]. The *Sc*CSN (*S. cerevisiae* CSN) is composed of 6 subunits, 4 PCI subunits (Csn9, Csn10/Rri2, Csn11/Pci8, Rpn5), one MPN subunit (Csn5/Rri1), and Csi1, a diverged homolog of Csn6 which does not contain recognizable domains [43, 80 – 81, 83-84]. Whereas CSN is essential for the development of organisms as different as plants (*A. thaliana*) and animals (*D. melanogaster*; *C. elegans*; mouse and human), budding yeast can survive without a CSN. Indeed, deletions of *CSN5* and *CSN9* genes show some increasing in pheromone sensitivity and mating efficiency [43]. More recently, neddylation of the budding yeast Cul1 (Cdc53) has been shown to be tightly regulated as noted upon carbon source shifting with possible metabolic implications [85]. These phenotypic effects, however, do not compromise budding yeast vitality. The non essentiality of CSN components and the availability of powerful genetic tools make *S. cerevisiae* a very promising model system to elucidate some aspects of its functions. Interestingly, Glickman and co-workers showed that CSN localization in *S. cerevisiae* is prevalently nuclear and that deletion of Csn12 leads to Csn5 delocalization to the cytoplasm [43]. To date, Csn12 is not considered a *Sc*CSN subunit but it could have a role in maintaining CSN integrity [43]. This observation opens up the perspective of a nuclear function of the CSN in *S. cerevisiae*, which could be related to chromatin organization and/or direct transcriptional control, as it is the case for the proteasomal lid [64 - 65], and as it has been suggested for CSN in other organisms [36].

2. AIM OF THE STUDY

The CSN is a multi-subunit protein complex conserved in all eukaryotes. The best characterized function is the regulation of the E3 ubiquitin ligase in the ubiquitin proteasome pathway. The catalytic activity of the CSN complex, carried by subunit 5 (Csn5), resides in the metal-binding domain that is responsible to remove a small ubiquitin-like protein called Nedd8 from the cullin. This function is important to regulate both the half-life of the proteins in the cell and the catalytic self-destruction of the CRLs. Whereas CSN- dependent CSN5 displays isopeptidase activity, it is intrinsically inactive in other forms. To date, the structure of the CSN from fungi to human is well-characterized. In multicellular eukaryotes the complex has been shown to regulate diverse cellular processes, ranging from cell-cycle progression and signal transduction to transcription regulation. Despite the increasing data about the CSN functions in the multicellular organisms, in budding yeast *S. cerevisiae* very few information are know about its functions. In *S. cerevisiae* the only described phenotype is that the deletion of some of its subunits show an increasing pheromone sensitivity and mating efficiency. In contrast to other eukaryotes, all the CSN components from budding yeast are non-essential. The non essentiality of CSN components and the availability of powerful genetic tools make *S. cerevisiae* a very promising model system to elucidate some aspect of its functions. In particular, we decided to look for a possible role of the *Sc*CSN on transcription.

We showed that Csn5 is involved in the modulation of the genes controlling aminoacid and lipid metabolism, and in particular the ergosterol biosynthesis. These alterations in gene expression correlate with the lower ergosterol levels and increased intracellular zinc content which we observed in *csn5* null mutant cells. The data have been obtained both by transcriptomic and proteomic approach. Our results, in particular the control of isoprenoid biosynthesis, are conserved through evolution as described previously in other eukaryotic organisms.

3. RESULTS

3.1 The Δ*csn5* mutant has defects in deneddylation and this phenotype can be rescued by exogenous Csn5

Null mutants of the budding yeast CSN, including the null of the enzymatic subunit Δ*csn5*, had been previously studied in the parental *BY4741* genetic background, and the lack of cullin de-neddylation had been described [43]. For this study, we have generated a new Δ*csn5* deletion mutant in the *W303* parental background. To confirm that this newly constructed mutant was also functional and affected in deneddylation, we have conducted an immunoblot analysis of total protein extracts from the mutants, using a commercial anti-Cdc53 antibody. Cdc53/Cul1 is one of the three cullins encoded by the *S. cerevisiae* genome [79]. Only the neddylated form of Cdc53 was observed in the lane corresponding to Δ*csn5*, indeed indicating a de-neddylation deficiency in this mutant (Fig. 5, panel A, lane 3). To further confirm that this was indeed due to absence of the *CSN5* gene, we monitored Cdc53 neddylation status also in Δ*csn5* cells transformed with a plasmid bearing wild-type *CSN5*, with its natural promoter, which showed a complete rescue of the de-neddylation activity (Fig. 5, panel A, lane 4 and 5). When the same experiment was conducted using a plasmid encoding a *CSN5* mutated in the catalytic JAMM domain, CSN de-neddylating activity could not be rescued (Fig. 5, panel A, lane 6). In addition, the lack of Csn5 did not affect either the levels of Csn9, genomically tagged by 13 repeats of Myc (Fig. 5 panel B, lane 2-4), or the levels of Rpn5, which is a shared subunit between the proteasome lid and the CSN complexes. Furthermore, lack of Csn5 did not lead to significant changes in the transcript expression of other CSN subunits, as compared to their relative wild type strain, suggesting that absence of Csn5 does not lead to changes in the levels of other CSN subunits (Fig. 5 panel C).

Still, it is not known whether the protein level of other subunits (Csn10, Csn11 and Csi1) is affected in Δ*csn5*.

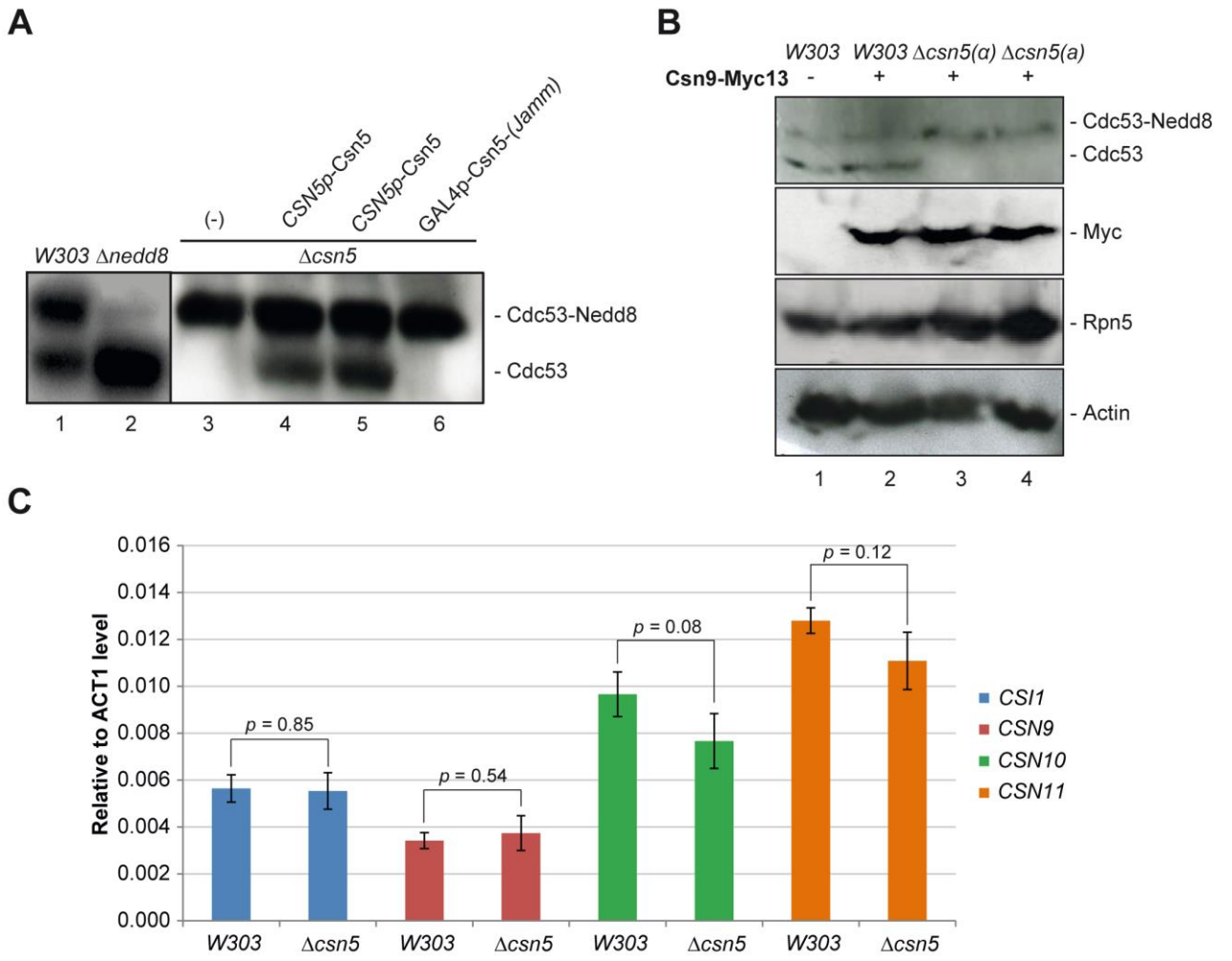

Fig. 5 *Δcsn5* yeast strain in the *W303* genetic context exhibits defects in deneddylation while expression levels of other complex subunits do not change significantly

Panel (A) De-neddylation assay. Yeast protein extracts of the *Δcsn5* strain, or *Δcsn5* complemented by plasmids, had been subjected to immunoblotting with the anti-Cdc53 antibody (Santa Cruz, CA). Wild type and *Δnedd8/Δrub1* (Lanes 1, 2) were added as size markers for the two forms of Cdc53 and Cdc53-Nedd8. See text for details.

Panel (B) Protein levels of Csn9 in the absence of Csn5. Yeast protein extracts of wild-type (lanes 1, 2) and *Δcsn5* strains expressing a genomic Csn9, tagged by 13Myc, were subjected to immunoblotting (lanes 2, 4). We also checked two different mating types (lanes 3, 4). Anti-Cdc53 has been used to confirm the mutants, and anti-actin as a loading marker. See text for details.

Panel (C) Expression levels of *CSI1*, *CSN9*, *CSN10*, *CSN11* in the absence of Csn5.
The data are the average of three independent experiments, error bars represent standard deviations and p values are obtained according to student T-test. See text for details.

3.2 Csn5 affects transcription of specific categories of genes

In order to gain a general view on the transcriptomic effects due to the absence of *CSN5*, we performed a genome-wide analysis using DNA microarrays containing the entire repertoire of *S. cerevisiae* ORFs. The mRNA profile of the Δ*csn5* strain was compared with its isogenic wild-type strain *W303*. Two independent cell cultures were analyzed for each strain. The microarray data derived from two biological replicates revealed that the expression levels of several *S. cerevisiae* genes were altered in the mutant compared with its isogenic wild-type (Table S1). We identified 2386 ORFs which gave reliable signals in both biological replicas for both strain (see Materials and Methods for filtering criteria). These data were subsequently used for functional analysis by the T-Profiler tool [86] (Table 1). This method scores changes in the average activity of pre-defined groups of genes and it does not require a pre-selected modulation cut-off in order to obtain a general view of transcriptomic regulation. Surprisingly, the results revealed that "Structural constituent of ribosome" was the most up-regulated functional category in the Δ*csn5* strain, being 123 genes of this category around 1.5 fold up-regulated compared with the wt (average log2 ratio = 0.67 and E-value<1.0×10^{-15}). Additionally, we found that 90 genes involved in the lipid metabolism category were down-regulated (average log2 ratio = -0.43 and E-value<3.42×10^{-5}).

Category	T-value	E-value	Log2 ratio *Δcsn5/W303*	N° ORFs
Structural costituent of ribosome	9.62	$<1.0\ e^{-15}$	0.666	123
Cytosolic ribosome (sensu Eukarya)	8.71	$<1.0\ e^{-15}$	0.643	110
Structural molecule activity	8.63	$<1.0\ e^{-15}$	0.498	173
Ribosome	7.96	$2.43\ e^{-13}$	0.500	149
Cytosolic large ribosomal subunit	7.87	$5.19\ e^{-13}$	0.798	61
Large ribosomal subunit	7.82	$7.78\ e^{-13}$	0.706	76
Ribonucleoprotein complex	6.89	$8.15\ e^{-10}$	0.364	204
Protein biosynthesis	6.09	$1.65\ e^{-7}$	0.299	233
Small ribosomal subunit	4.14	$5.06\ e^{-3}$	0.456	53
Ergosterol biosynthesis	-3.63	$4.05\ e^{-2}$	-0.752	17
Carbohydrate transporter activity	-4.12	$5.52\ e^{-3}$	-0.994	13
Response to inorganic substance	-4.26	2.98 e-^{3}	-1.526	7
Fructose transporter activity	-4.38	$1.73\ e^{-3}$	-1.433	8
Hexose transport	-4.54	$8.21\ e^{-4}$	-1.373	9
Lipid metabolism	-5.17	$3.42\ e^{-5}$	-0.434	90

Tab. 1 Functional categories which are globally modulated in the *Δcsn5* strain as compared with the isogenic wt strain.
T-value and E-value were calculated as described in [86]. T-value >1 indicates the gene categories that are upregulated; T-value <1 gene categories downregulated.
We selected 2386 ORFs, Mean 0.0, Stddev. 0.8.

In particular, down-regulated genes within last category included most of the genes involved in the biosynthesis of fungal sterol ergosterol (Fig. 6). We used the same tool also to score groups of genes whose promoters have been previously shown to bind in vivo particular transcription factors by Chromatin Immunoprecipitation associated with microarray technology (ChIP on chip) analysis [87] and showing a significant average up- or down-regulation (Table 2). Our experimental conditions revealed that around 100 genes which bind Rap1 and/or Fhl1 *in vivo* were in average 1.5 fold up-regulated in the Δ*csn5* as compared with wt, (E-value<2.12×10^{-6} and E-value<1.0×10^{-15}, respectively), while 71 Hap1-target genes were in average 1.35 fold down-regulated ($P<1.21 \times 10^{-4}$). Down-regulation of Hap1 binding genes is particularly intriguing, since this transcription factor is known to be activated by high concentration of heme which shares with the ergosterol biosynthesis pathway Farnesyl Pyrophosphate (FPP) as precursor [88].

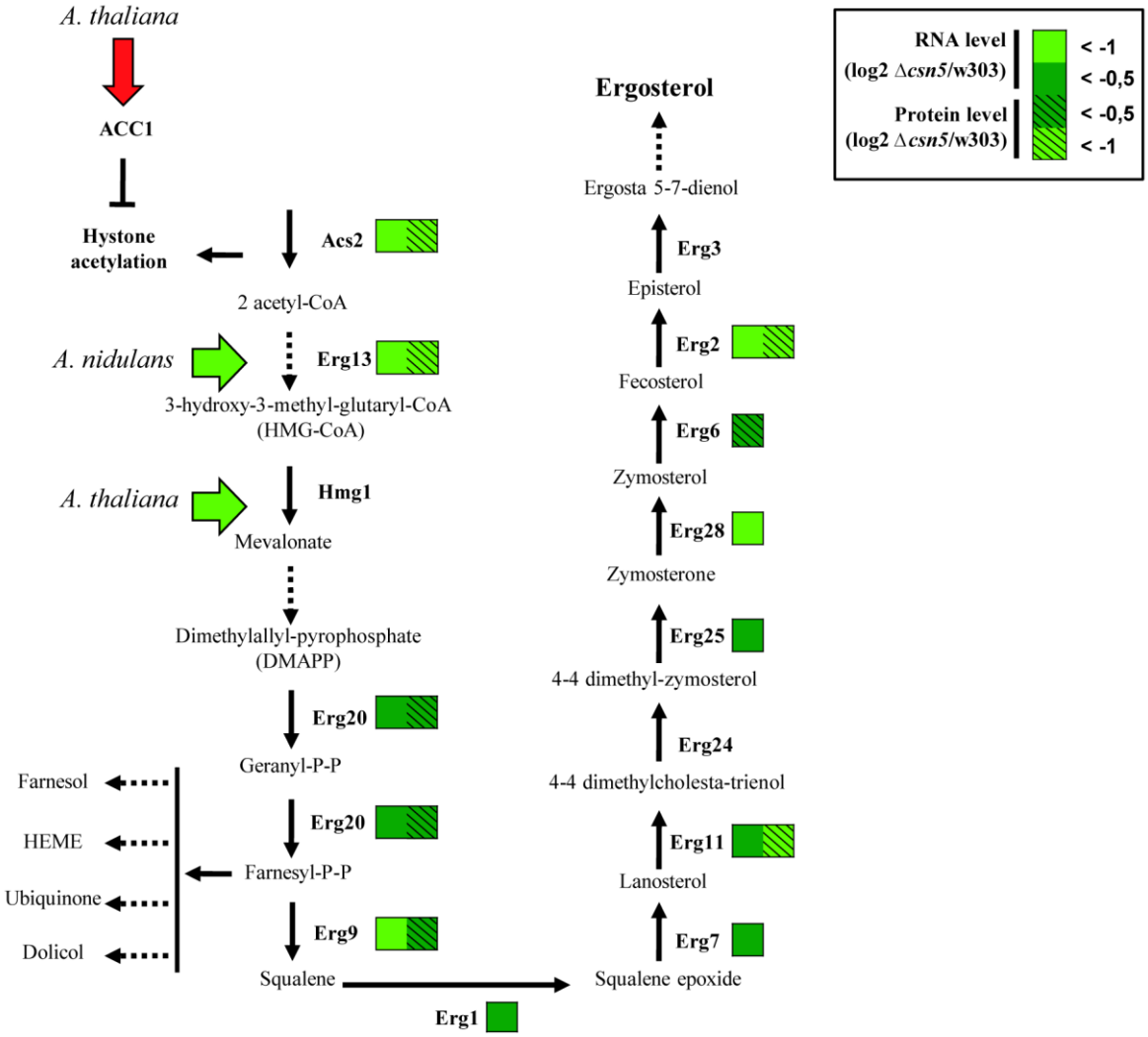

Fig. 6 The Csn is involved in the control of the pathways of acetyl-CoA utilization.
Schematic representation of the biosynthetic pathway of isoprenoids and ergosterol. Broken arrows indicate multiple enzymatic steps. Genes coding for enzymes of this pathway and modulated at the RNA and/or at the protein level in the Δ*csn5* strain are indicated with different kinds of green boxes. A legend is provided on the right. Red and green arrows represent inductions and repressions, respectively, observed in other eukaryotic organisms.

Protein	Condition	t-value	E-value	Mean	N° ORFs
Flh1	YPD	9.55	$<1.0\ e^{-15}$	0.696	112
Rap1	YPD	5.80	$2.12\ e^{-6}$	0.461	97
Hap1	YPD	-5.08	$1.21\ e^{-4}$	-0.484	71

Tab. 2 Number of ORFs found modulated in Δ*csn5* and whose promoters are known to be bound in vivo by specific transcription factors.
List of known in vivo targets of the transcription factors Flh1, Rap1 and Hap1 found also to be significantly modulated in Δ*csn5* cells, when compared to the isogenic wild type.
T-value and E-value were calculated as described in [86]. (ChIP on chip data, see ref [87])

Several gene modulations were further validated by real time RT-PCR (Fig. 7). We selected two genes involved in ergosterol biosynthesis (*ERG2* and *ERG28*), one gene involved in lipid biosynthesis (*FAA4*), a gene known as a modulator of cullin activity (*SCM4*) [89], and a series of genes involved in zinc metabolism (*ZRT1*, *ZRT2*, *IZH1*, *IZH2* and *IZH4*), which were all down-regulated in Δ*csn5* cells. As shows Fig.7, there is an excellent correlation between the real time RT-PCR and the microarray data (Pearson's r correlation = 0.92; p-value = 1.6×10^{-5}). The genes involved in zinc metabolism were previously showed to be under the control of transcription factor Zap1 [90]. We could not obtained reliable data for *ZAP1* mRNA accumulation by DNA microarrays due to its low level of expression but real time RT-PCR showed a significant reduction in the Δ*csn5* strain (Fig. 8, panel A). Furthermore, we also tested a couple of induced genes involved in the autophagy pathway (*ATG16* and *ATG33*, Fig. 8 panel B). Next, we tested the expression of selected genes in strains deleted in other subunits of the *Sc*CSN complex (Csn9, Csn10/Rri2, and Csn11/Pci8 and Csi1; Fig. 8 panel C and panel D). Similar modulations of transcript levels were also observed in these strains, suggesting that the changes in gene expression observed in the Δ*csn5* mutant were caused by a defect in the function of the whole complex, rather than being linked to a missing function of the single Csn5 protein.

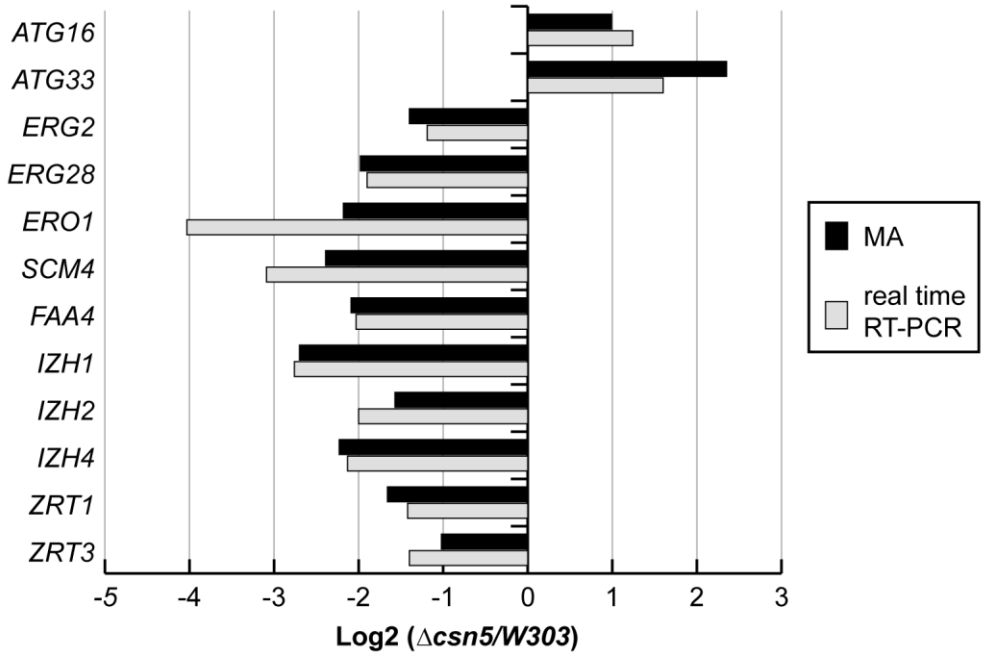

Fig. 7 Validation of some modulated genes in Δ*csn5* cells by real time RT-PCR

The bar plot shows the average modulation of the indicated genes as measured by DNA microarrays analysis (MA) or real time RT-PCR (at least two independent experiments, original data are shown in Figure 8 panel A).

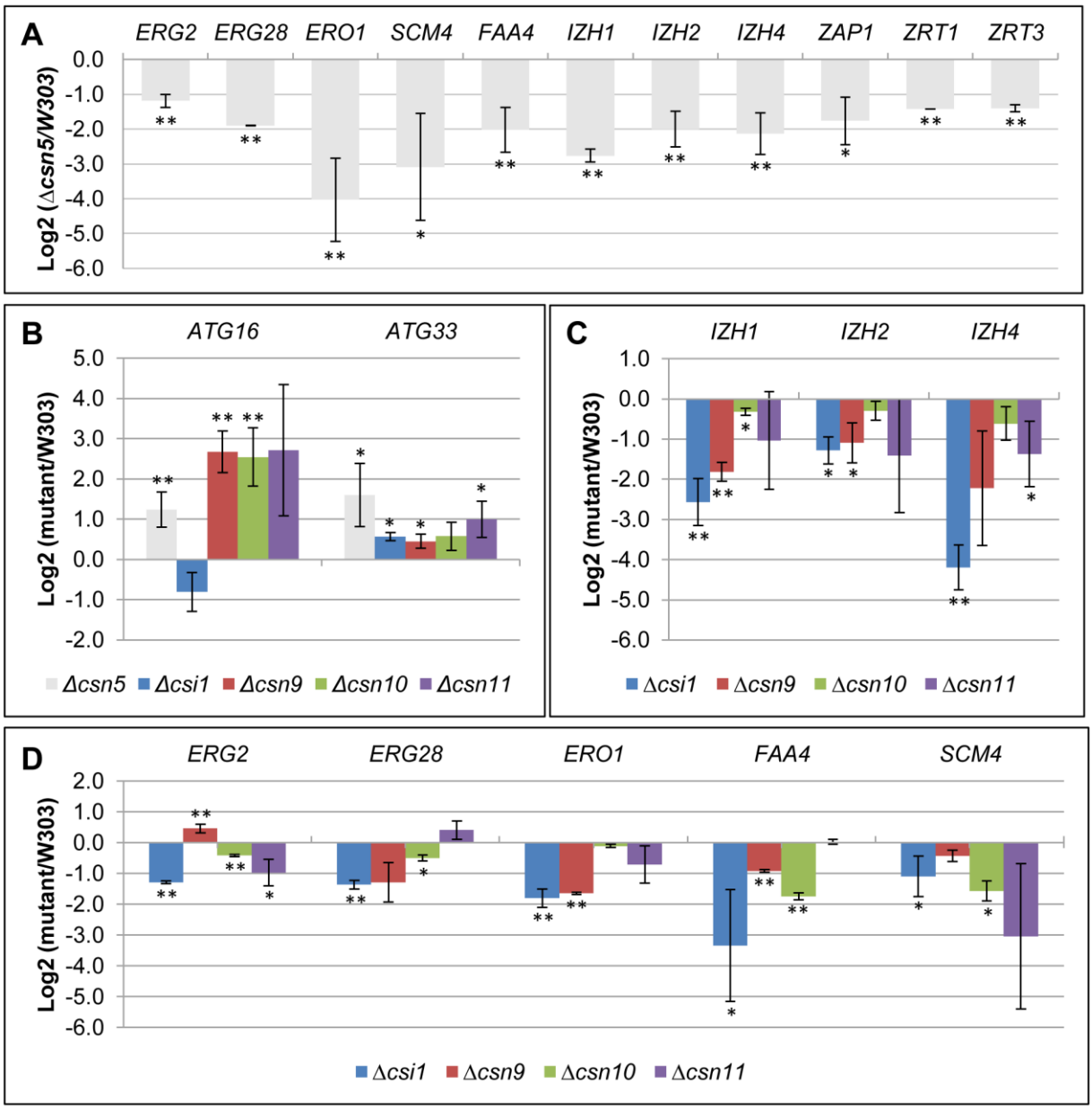

Fig. 8 Testing gene modulation in strains deleted for CSN components by real time RT-PCR
Panel A Validation of the modulations observed in the Δ*csn5* strain. The histograms show Log2 ratios between Δ*csn5* and the *W303* strain for 11 genes down-regulated according to microarray experiments. *ACT1* was used as endogenous calibrator. The data are the average of at least two independent experiments, bars represent standard deviations; asterisks show p values obtained according to student T-test: * <0.05; **<0.01.
Panel B Testing the expression of two up-regulated genes in strains deleted for CSN components by real time RT-PCR. The histograms show Log2 ratios between the indicated deleted strains and the isogenic WT strain for *ATG16* and *ATG33*. *ACT1* was used as endogenous calibrator. Δ*csn5*, Δ*csi1*, Δ*csn9*, Δ*csn10 and* Δ*csn11* are strains deleted in Csn5/Rri1, Csi1, Csn9, Csn10/Rri2 and Csn11/Pci8, respectively. The data are the average of at least two independent experiments, bars represent standard deviations.
Asterisks show p values obtained according to student T-test: * <0.05; **<0.01..
Panel C As in B for *IZH1*, *IZH2* and *IZH4*.
Panel D As in B for *ERG2, ERG28, ERO1, FAA1* and *SCM4*.

The heat map represented in Fig. 9 summarizes real-time RT-PCR data obtained in all CSN components deleted strains.

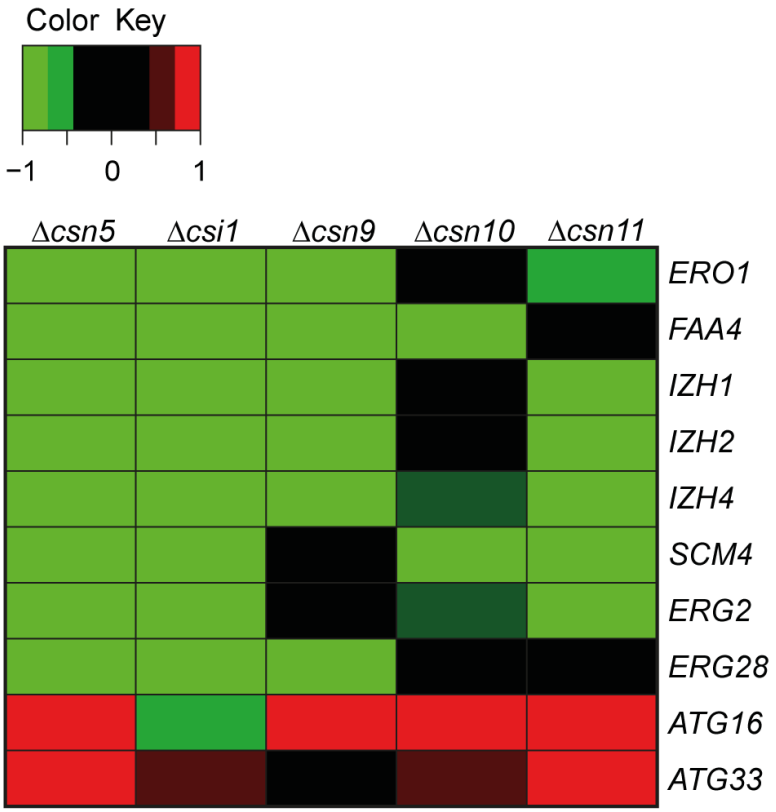

Fig. 9 Validation of some modulated genes in Δ*csn5* cells by real time RT-PCR

The transcriptional modulations observed in Δ*csn5* strain are also found in strains deleted in other CSN components. The heat map summarizes real-time RT-PCR data (see Fig. 8) obtained in the indicated strains deleted in other yeast CSN components. Data are the average of at least two independent experiments.

3.3 The proteome of the Δ*csn5* strain partly recapitulates the transcriptome

Since the transcriptomic alterations observed in the Δ*csn5* mutant appeared reproducible and coherent, we decided to verify if they corresponded to similar variations in protein abundance by analyzing the genome-wide proteome of the Δ*csn5* strain using a label-free shotgun approach (see Materials and Methods). We analyzed total protein extracts purified from four independent cultures for each strain, run simultaneously. Samples from the same strains exhibited a high level of correlation excluding that the observed modulation could be the consequence of technical artefacts (Fig. 10). We obtained reliable data for approximately 750 proteins (see Materials and Methods).

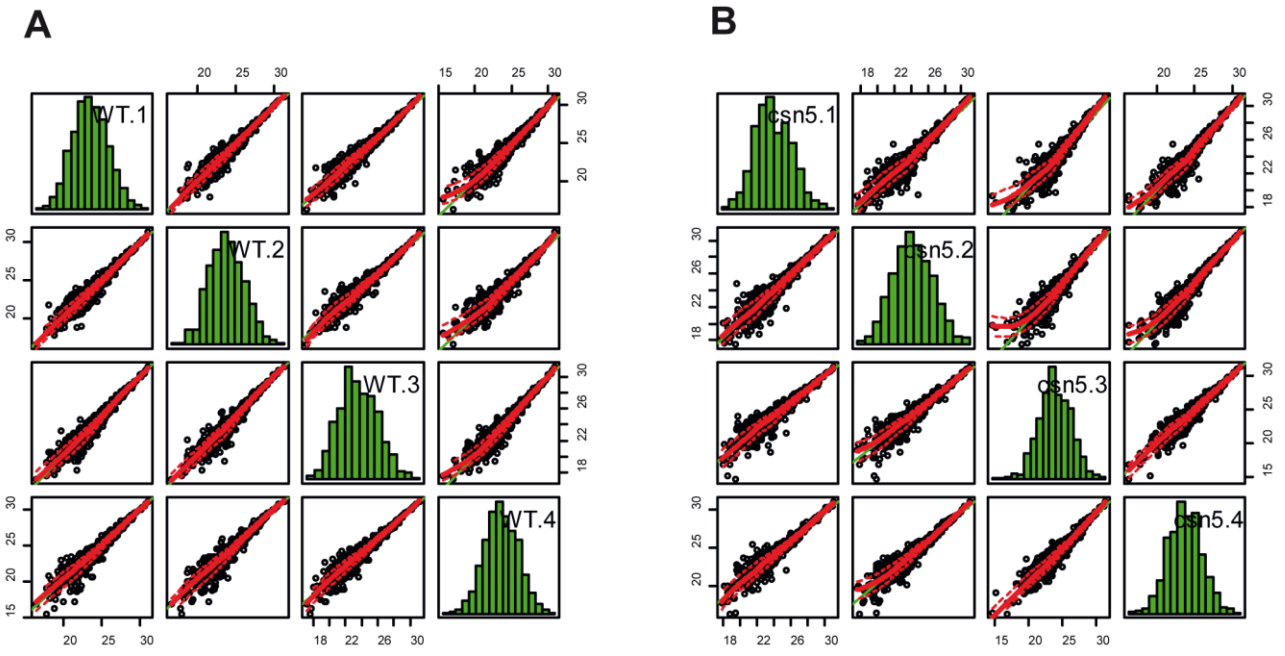

Fig. 10 Histogram distributions and pair wise correlation plots for the label-free quantification proteomic data of the four wt strains (panel A) and four *Δcsn5* strains (panel B)

Among them, 106 showed quantitative and reproducible changes in their levels (false discovery rate (FDR) cut-off of 20%, see Table 3).

Protein ID	Gene Name	Log2 ratio Δ*csn5/W303*	FDR < 0.05	FDR < 0.10	p-value
YGL009C	LEU1	-2.67	+	+	3.9 e^{-06}
YMR202W	ERG2	-1.99		+	6.9 e^{-03}
YNR050C	LYS9	-1.95	+	+	1.2 e^{-05}
YPL028W	ERG10	-1.67			1.6 e^{-02}
YKL029C	MAE1	-1.50	+	+	4.7 e^{-03}
YBR115C	LYS2	-1.44		+	1.1 e^{-02}
YDR487C	RIB3	-1.34			2.5 e^{-02}
YKR071C	DRE2	-1.31			4.2 e^{-02}
YHR007C	ERG11	-1.30			2.6 e^{-02}
YLR153C	ACS2	-1.29	+	+	3.2 e^{-03}
YEL055C	POL5	-1.28			3.5 e^{-02}
YML126C	ERG13	-1.20	+	+	1.2 e^{-04}
YHR208W	BAT1	-1.11	+	+	1.2 e^{-05}
YLR003C	CMS1	-1.04			2.9 e^{-02}
YJR125C	ENT3	-1.03			1.4 e^{-02}
YPL217C	BMS1	-1.02			3.4 e^{-02}
YIL094C	LYS12	-1.02	+	+	2.4 e^{-03}
YHR009C	TDA3	-1.01			3.9 e^{-02}
YJL200C	ACO2	-1.00	+	+	9.8 e^{-05}
YPR191W	QCR2	-0.98			4.4 e^{-02}
YGR234W	YHB1	-0.95			3.1 e^{-02}
YBL002W	HTB2	-0.92			1.8 e^{-02}
YDR502C	SAM2	-0.90	+	+	2.1 e^{-04}
YJL167W	ERG20	-0.89			2.3 e^{-02}
YHR190W	ERG9	-0.88			4.3 e^{-02}
YEL034W	HYP2	-0.86	+	+	2.2 e^{-04}
YMR309C	NIP1	-0.85			4.0 e^{-02}
YKR043C	SHB17	-0.78			2.4 e^{-02}
YPL235W	RVB2	-0.77		+	1.3 e^{-02}
YNR043W	MVD1	-0.76	+	+	2.5 e^{-03}
YDL182W	LYS20	-0.73	+	+	3.7 e^{-03}
YOR198C	BFR1	-0.73			1.4 e^{-02}
YOR375C	GDH1	-0.72	+	+	1.1 e^{-03}
YPR060C	ARO7	-0.71		+	1.0 e^{-02}
YOL039W	RPP2A	-0.70	+	+	9.8 e^{-04}
YML008C	ERG6	-0.69		+	6.0 e^{-03}
YKL127W	PGM1	-0.65			4.2 e^{-02}
YER091C	MET6	-0.64	+	+	1.6 e^{-03}
YMR108W	ILV2	-0.64			2.0 e^{-02}

YDR382W	RPP2B	-0.62			$3.2\ e^{-02}$
YJL012C	VTC4	-0.61	+	+	$1.9\ e^{-04}$
YDL131W	LYS21	-0.60			$4.3\ e^{-02}$
YDR529C	QCR7	-0.56		+	$1.0\ e^{-02}$
YLR355C	ILV5	-0.53	+	+	$2.6\ e^{-04}$
YER043C	SAH1	-0.53	+	+	$2.5\ e^{-04}$
YER055C	HIS1	-0.41			$2.2\ e^{-02}$
YIL020C	HIS6	-0.41			$2.2\ e^{-02}$
YHR089C	GAR1	-0.40			$2.3\ e^{-02}$
YBL003C	HTA2	-0.35		+	$8.1\ e^{-03}$
YHL001W	RPL14B	-0.33			$2.6\ e^{-02}$
YNL055C	POR1	-0.28			$2.3\ e^{-02}$
YKL182W	FAS1	-0.27	+	+	$3.3\ e^{-03}$
YDL083C	RPS16B	-0.26			$4.4\ e^{-02}$
YNL104C	LEU4	-0.23		+	$1.1\ e^{-02}$
YLR044C	PDC1	-0.19			$1.6\ e^{-02}$
YJR121W	ATP2	-0.18			$4.4\ e^{-02}$
YLL045C	RPL8B	-0.18	+	+	$4.0\ e^{-03}$
YHR203C	RPS4B	0.08			$3.3\ e^{-02}$
YLR167W	RPS31	0.18			$2.9\ e^{-02}$
YDL185W	VMA1	0.19		+	$6.4\ e^{-03}$
YGR034W	RPL26B	0.21			$1.4\ e^{-02}$
YER074W	RPS24A	0.22			$1.4\ e^{-02}$
YHR019C	DED81	0.24			$3.9\ e^{-02}$
YER009W	NTF2	0.25			$2.1\ e^{-02}$
YBR118W	TEF2	0.28			$1.6\ e^{-02}$
YDL192W	ARF1	0.28		+	$9.4\ e^{-03}$
YGR155W	CYS4	0.31			$3.1\ e^{-02}$
YBL076C	ILS1	0.32			$2.8\ e^{-02}$
YGL026C	TRP5	0.33			$3.2\ e^{-02}$
YOR063W	RPL3	0.35			$4.2\ e^{-02}$
YGR254W	ENO1	0.36			$2.5\ e^{-02}$
YGR240C	PFK1	0.36		+	$5.8\ e^{-03}$
YFR031C-A	RPL2A	0.36	+	+	$3.2\ e^{-03}$
YLR109W	AHP1	0.37			$2.2\ e^{-02}$
YAL038W	CDC19	0.38	+	+	$3.7\ e^{-04}$
YLR447C	VMA6	0.39			$1.7\ e^{-02}$
YBR121C	GRS1	0.39			$3.7\ e^{-02}$
YER070W	RNR1	0.41			$4.4\ e^{-02}$
YHR141C	RPL42B	0.41			$4.0\ e^{-02}$
YGL148W	ARO2	0.41			$1.5\ e^{-02}$
YLR287C-A	RPS30A	0.42			$3.5\ e^{-02}$
YPL106C	SSE1	0.42		+	$1.2\ e^{-02}$
YHR179W	OYE2	0.48			$3.9\ e^{-02}$
YMR072W	ABF2	0.51	+	+	$3.6\ e^{-03}$
YDR002W	YRB1	0.53			$2.5\ e^{-02}$
YKL081W	TEF4	0.53		+	$5.9\ e^{-03}$
YGL008C	PMA1	0.54			$2.1\ e^{-02}$
YAR071W	PHO11	0.54		+	$7.8\ e^{-03}$

YDR033W	MRH1	0.55			1.3 e^{-02}
YHR068W	DYS1	0.58			1.3 e^{-02}
YPR074C	TKL1	0.59			1.8 e^{-02}
YIL051C	MMF1	0.60			3.5 e^{-02}
YGR180C	RNR4	0.63	+	+	4.7 e^{-04}
YBR048W	RPS11B	0.65	+	+	4.4 e^{-03}
YBR078W	ECM33	0.67	+	+	5.0 e^{-03}
YBR263W	SHM1	0.70			1.7 e^{-02}
YBL039C	URA7	0.72		+	6.2 e^{-03}
YGR185C	TYS1	0.73			3.7 e^{-02}
YNR001C	CIT1	0.73		+	1.2 e^{-02}
YLR304C	ACO1	0.75	+	+	6.5 e^{-04}
YBR218C	PYC2	0.76			4.3 e^{-02}
YOR168W	GLN4	0.79			3.5 e^{-02}
YGR037C	ACB1	0.86			1.9 e^{-02}
YOL059W	GPD2	0.88			2.0 e^{-02}
YLR300W	EXG1	0.92			2.1 e^{-02}
YER052C	HOM3	0.92			4.1 e^{-02}
YER136W	GDI1	0.93	+	+	2.0 e^{-03}
YJL052W	TDH1	0.96		+	7.3 e^{-03}
YMR318C	ADH6	0.98		+	1.2 e^{-02}
YDR032C	PST2	1.02			1.7 e^{-02}
YOR341W	RPA190	1.03		+	5.8 e^{-03}
YER025W	GCD11	1.08			1.6 e^{-02}
YLR342W	FKS1	1.12		+	7.1 e^{-03}
YOR151C	RPB2	1.12			1.8 e^{-02}
YEL047C	FRD1	1.13		+	1.1 e^{-02}
YJL130C	URA2	1.17	+	+	1.8 e^{-04}
YAL044C	GCV3	1.21			1.8 e^{-02}
YDR324C	UTP4	1.27		+	1.1 e^{-02}
YDL195W	SEC31	1.30			4.5 e^{-02}
YBR072W	HSP26	1.36	+	+	1.2 e^{-04}
YLR250W	SSP120	1.41			3.2 e^{-02}
YDR258C	HSP78	1.54		+	1.0 e^{-02}
YLR179C		1.82	+	+	1.2 e^{-03}
YEL071W	DLD3	2.26	+	+	6.3 e^{-04}
YHR137W	ARO9	3.21	+	+	5.6 e^{-04}
YIR037W	HYR1	3.26	+	+	4.0 e^{-04}
YDR380W	ARO10	3.43	+	+	5.4 e^{-07}

Tab. 3 Modulated proteins in the *Δcsn5* strain as compared with the isogenic wt strain.
Values represent the average of four independent extracts for each strain. Values with FDR<0.20 are reported and values with FDR<0.05 and FDR<0.10 are marked with '+'.

An analysis of these modulated proteins showed a correlation between transcriptomic and proteomic analyses of enzymes involved in ergosterol biosynthesis, such as Erg2, Erg6, Erg9, Erg11 and Erg20. These enzymes are down-regulated at the mRNA level (Fig. 6), and less abundant at the protein level (Table 3). However, a positive correlation between the two sets of data was not always found (Table 4).

Systematic Name	Gene Symbol	mRNA	Protein
YDL083C	RPS16B	0.66	-0.26
YOL039W	RPP2B	0.77	-0.70
YHL001W	RPL14B	0.73	-0.33
YLR287C-A	RPS30A	2.75	0.42
YOR063W	RPL3	0.69	0.35
YER074W	RPS24A	1.27	0.22
YHR141C	RPL42B	2.97	0.41
YEL047C	FRD1	-1.19	1.13
YGR037C	ACB1	-0.98	0.86
YGR185C	TYS1	-0.43	0.73
YGR254W	ENO1	-0.72	0.36
YHR007C	ERG11	-0.64	-1.30
YHR190W	ERG9	-1.21	-0.88
YKR071C	DRE2	-0.85	-1.31
YLR109W	AHP1	-0.91	0.37
YMR202W	ERG2	-1.40	-1.99
YNL104C	LEU4	-0.49	-0.23
YOL059W	GPD2	-1.27	0.88
YOR063W	RPL3	0.69	0.35
YOR375C	GDH1	-0.67	-0.72
YPL106C	SSE1	-0.79	0.42
YEL034W	HYP2	-1.46	-0.86
YLR153C	ACS2	-1.59	-1.29
YGL009C	LEU1	-0.91	-2.67
YML126C	ERG13	-1.11	-1.20
YHR208W	BAT1	-0.74	-1.11
YER091C	MET6	0.94	-0.69
YDR380W	ARO10	-1.31	3.43
YHR137W	ARO9	-0.61	3.21
YGR180C	RNR4	-1.18	0.63
YJR125C	ENT3	-0.68	-1.03
YDL182W	LYS20	0.64	-0.73
YKL081W	TEF4	0.80	0.53
YGR234W	YHB1	-1.43	-0.95
YBL002W	HTB2	-0.98	-0.92
YJL167W	ERG20	-0.83	-0.89
YGR137C	ACB1	-1.45	0.86

YOR168W	GLN4	0.65	0.79

Tab. 4 List of 38 regulated genes in the Δ*csn5* as compared with the isogenic wt strain at RNA and/or protein level. Values represent the average Log2 ratio Δ*csn5/W303*. Genes with coordinated regulation are marked in yellow in the first and second column. Values are marked in bright green (<-0.5); dark green (<0>-0.5); orange (>0<0.5); red (>0.5).

As an example, proteins involved in aminoacid metabolism, such as Aro9 and Aro10, are more abundant in the Δ*csn5* mutant, while their respective mRNAs are modestly down-regulated. Similarly, the thiol peroxidase Hyr1 is more abundant at the protein level, while the respective mRNA level does not change in Δ*csn5*, if compared with the wild-type. On the other hand, similarly to what was observed at the RNA level, the fraction of proteins whose abundance is lower in Δ*csn5* is highly enriched in proteins encoded by genes known to be bound by the Hap1 transcription factor in cells grown in rich medium (Tab. 5). An important complementation of this study would be the analysis of the above mentioned proteins half-life time, in the context of Csn5 deficiency.

Systematic Name	**Gene Symbol**	**Log2 ratio (Δ*csn5/W303*)**
YMR202W	ERG2	-1.99
YPL028W	ERG10	-1.67
YHR007C	ERG11	-1.3
YLR153C	ACS2	-1.29
YML126C	ERG13	-1.20
YGR234W	YHB1	-0.95
YHR190W	ERG9	-0.88
YEL034W	YHYP2	-0.86
YNR043W	MVD1	-0.76
YML008C	ERG6	-0.69
YDR529C	QCR7	-0.56
YKL182W	FAS1	-0.27
YLR109W	AHP1	0.37

Tab. 5 Genes modulated at protein level whose promoter has been shown to bind Hap1 in YPD by ChIP on chip experiments. Values represent the average log2 ratio Δ*csn5/W303*

3.4 The Δ*csn5* mutant has reduced ergosterol content

Comparative analysis of the transcriptome and proteome suggested a significant impact of Csn5 on ergosterol biosynthesis. Because absence of Csn5 leads to down-regulation of several enzymes of the ergosterol biosynthesis regulon, it can be predicted that, as a consequence, the overall ergosterol biosynthesis may be affected. To verify this hypothesis, we measured the ergosterol content in the Δ*csn5* mutant cells by Gas Chromatography (GC) analysis. Table 6 shows that the Δ*csn5* strain shows a significant (25%) reduction in the ergosterol content as compared with the isogenic wild type. We further confirmed this finding by assessing the ability of the Δ*csn5* mutant to grow in the presence of nystatin and ketoconazole. Nystatin targets ergosterol in the cell membrane, while ketoconazole interferes with ergosterol biosynthesis [91]. Appropriately, the results shown in Table 6 indicate that Δ*csn5* cells are indeed more sensitive to ketoconazole and more resistant to nystatin as compared with the wt, again confirming an alteration in ergosterol biosynthesis. The ergosterol reduction observed in the Δ*csn5* strain is within the same range (12 - 51%) observed in yeast cells treated with different azole derivatives at sub-inhibitory concentrations (0.01-1 mM/L) [92 - 93]. At higher azole concentrations (3 - 10 mg/ml), a further decrease in ergosterol is observed in these cells, accompanied by a decrease in chitin levels and by an evident cytostatic activity. This explains why the *CSN5* deleted strain shows higher sensitivity to ketoconazole, although it can still grow efficiently in normal conditions.

Strain	Ergosterol content	Nystatin	Ketoconazol
W303	3.27 mg/mg dried weight	sensitive to 6 u/ml	sensitive to 4mg/ml
Δ*csn5*	2.43 mg/mg dried weight	sensitive to 24 u/ml	sensitive to 1mg/ml

Tab. 6 Ergosterol content and related phenotypes for the *Δcsn5* strain compared with the isogenic *W303* strain.

3.5 Δ*csn5* mutants have alterations in transition metals uptake

A reduced content of ergosterol in the cell membrane has previously been linked with an increased permeability to mono and divalent cations [94 - 95] in general and to metal cations in particular [94]. Indeed, our transcriptomic analysis showed repression of several genes coding for key regulators of Zn metabolism (Fig. 7), such *ZRT1*, *ZRT3*, *IZH1*, *IZH2*, *IZH4* and of *ZAP1*, which encodes their transcription activator (Fig. 10).

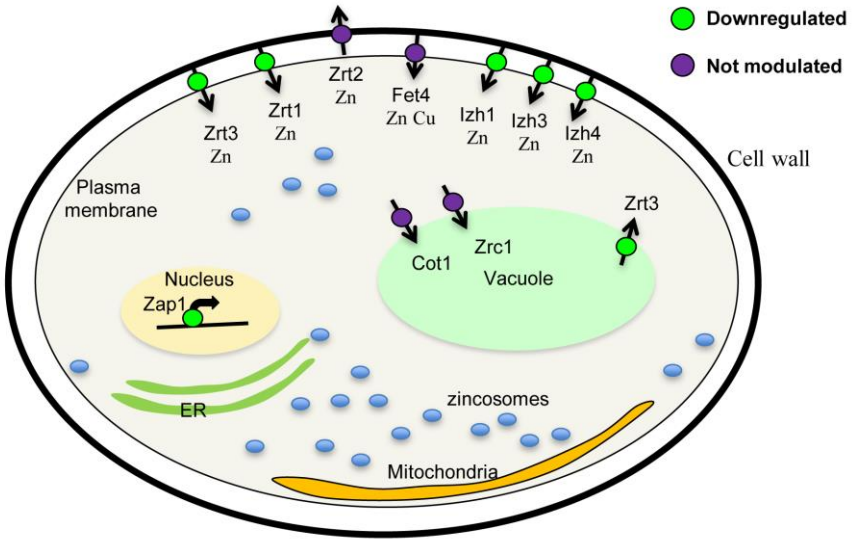

Fig. 10 Overview of the zinc transporters and zinc metabolism genes repressed in *Δcsn5* cells. Representation showing the genes involved in the zinc import and metabolism in *S. cerevisiae* [90] and their modulation in the *Δcsn5* strain.

This alteration in gene expression could be caused by an increased content of Zn in the cytoplasm. To verify if the low expression of zinc metabolism genes observed in Δ*csn5* cells could be correlated to an alteration in Zn content, we checked Zn intracellular levels using the fluorescent dye called zinquin ethyl ester (see Material and Methods). This Zn-specific dye has been already used successfully to measure relative zinc levels in *S. cerevisiae* [96 - 97]. While poor zinquin staining was observed in wild type cells grown under normal conditions, addition of 500 μM of $ZnSO_4$ to the medium resulted in the formation of small, bright fluorescent granules (zincosomes) (Fig. 10). Several zincosomes are instead already present in the cytoplasm of the Δ*csn5* strain in

normal conditions and they further increase upon addition of 500 μM of $ZnSO_4$ to the medium. Zincosomes appear mainly localized around the vacuoles, suggesting that besides an increased passive import in the cell, the deleted strain shows also a defective import and storage in the vacuole. A similar increased permeability to zinc is observed in a strain deleted in *ERG6* (Fig. 11), confirming a direct relationship between ergosterol deficit and passive zinc income.

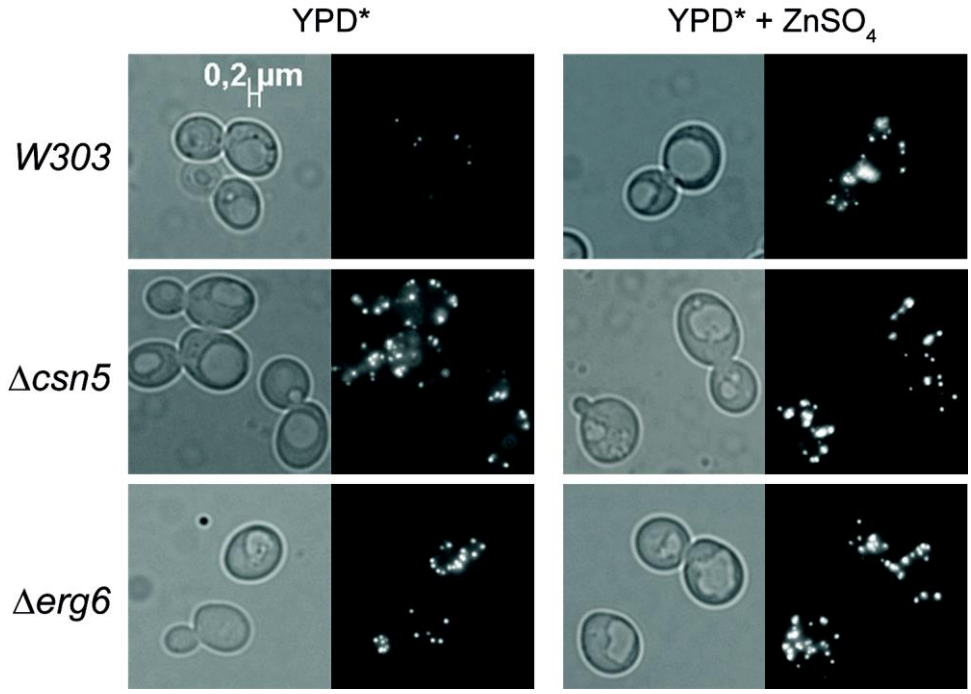

Fig. 11 Zinquin staining reveals zinc accumulation in the *Δcsn5* strain
The indicated strains were grown overnight to saturation in YPD* (see Materials and Methods), 500 μM of $ZnSO_4$ was added where indicated. Zinc-rich vescicles were visualized by zinquin staining.

We also tested the growth yield of the Δ*csn5* strain and of its isogenic wild-type strain in a Limiting Zinc Medium (LZM) containing different zinc concentrations (see Material and Methods). Indeed, the growth of the Δ*csn5* is slower at low Zn concentration, as compared with its isogenic wild type (Fig. 12 panel A). This growth defect was rescued only at concentrations above 500 μM of $ZnSO_4$, a Zn concentration at which active import is probably less stringent. Ectopic expression of the *CSN5*

gene was sufficient to restore efficient growth at a low Zn concentration (Fig. 12 panel B).

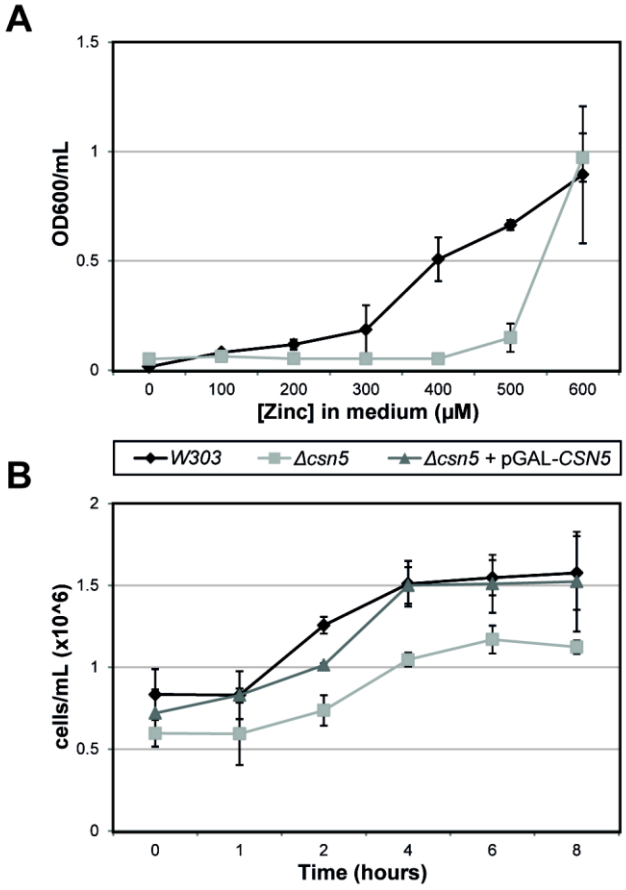

Fig. 12 The *Δcsn5* strain shows a growth defect in low zinc which can be suppressed by ectopic expression of *CSN5*.

Panel (A) The same amount of cells (0,02 OD600/mL) of wild-type *W303* and *Δcsn5* were inoculated into LZM (as described in Material and Methods) supplemented with the indicated amount of $ZnSO_4$ (0-600µM) and grown for 16 hr prior to cell number determination (OD).
Shown are the mean values of three independent experiments.
Panel (B) The same amount of cells of wild-type *W303*, *Δcsn5* and *Δcsn5* + pGAL-*CSN5* strains were inoculated into LZM (as described in Material and Methods) supplemented with 500 µM of $ZnSO_4$ and grown at indicated hours. The cell number determination (OD) was measured at indicated hours.
Shown are the mean values of three independent experiments.

We extended our analysis also to other transition metals and found a slower growth of the Δ*csn5* strain as compared with the isogenic wild type in metal deprived medium supplemented with limiting concentrations of cadmium or nickel (Fig. 13). We interpret these results as an indication of a less efficient active import of metal cations in the Δ*csn5* strain which could be related to

transcriptional repression of *ZRT1* and *FET4* transporters which we observed in the mutant strain.

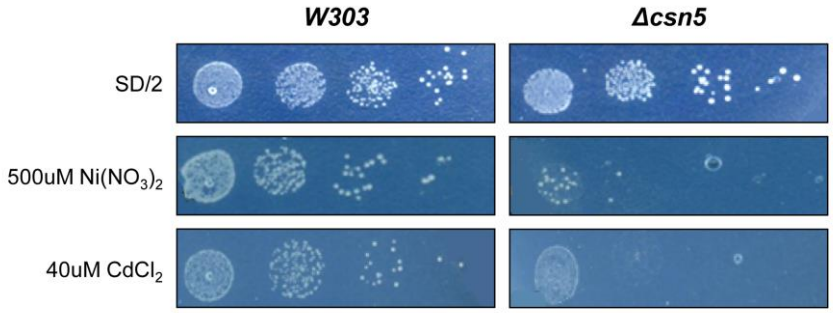

Fig.13 *Δcsn5* mutant cells are sensitive to cadmium and nickel
The growth of wild type (*W303*) strain on SD/2 on either nickel or cadmium as compared with *Δcsn5* strain growth that is inhibited at the same concentrations. Serial dilutions of *W303* and *Δcsn5* mutant cells were plated on SD/2 (half synthetic define), supplemented with either $CdCl_2$ or $Ni(NO_3)_2$ at the indicated concentration.

4. DISCUSSION

In this study, we have deciphered the transcriptomic and proteomic modulations of the budding yeast *Δcsn5* in the *W303* genetic context. We show that the deletion of *CSN5* in buddying yeast does not change the mRNA level of other CSN subunits, nor the protein level of Csn9 (Fig. 5, panel B and C). On the other hand, our results demonstrate that Csn5 is able to regulate, directly or indirectly, several sets of genes and proteins.

First, we observed a general up-regulation of genes coding for components of the protein biosynthetic apparatus (Table 1), including genes coding for at least 26 ribosomal proteins (RP). These genes are known to be mainly controlled by the Rap1 and Fhl1 transcription factors. Interestingly, similar genes were also found to be regulated by CSN in other eukaryotic organisms. For example, in *A. thaliana*, Ma et al. [98] previously found a general up-regulation of genes coding for at least 29 RP genes mRNAs in dark-grown csn8 (cop9-1) mutant seedlings. The same genes were even more strongly up-regulated in dark-grown cop10-1 (a mutant in an ubiquitin E2 variant) seedlings, suggesting that the regulation of their expression might involve CSN and its ubiquitin ligase-mediated regulation of specific transcription factors or of proteins involved in mRNA stability. Indeed, the results from our proteomic analysis show that in *S. cerevisiae* the CSN-mediated regulation of these genes remains substantially confined at the mRNA level, since only four of the transcriptionally upregulated RPs (*RPL3, RPL42B, RPS24A* and *RPS30A*) are found significantly increased also at the protein level, while three of them (*RPP2B, RPL14B* and *RPL16B*) are instead found significantly decreased at the protein level (Table 4). It is likely that, in the *Δcsn5* mutant, a translational negative control partly compensates the RP mRNA accumulation. It has been previously shown that several mammalian RPs are selectively neddylated [99] and therefore potentially less stable in the *Δcsn5*; yet, so far the link between this neddylation and the CSN complex, had not been confirmed. In this case, this transcriptional up-regulation could represent a feedback compensation mechanism.

Second, most of the genes that are involved in lipid biosynthesis are down-regulated in *Δcsn5* cells (Table 1). This is reflected at the phenotypic level by a reduction of the ergosterol content and by an increased sensitivity and resistance to ketoconazole and to nystatin, respectively. Interestingly, the group of down-regulated gene includes about 70 genes which are known to be bound and regulated by the transcription factor Hap1. This is particularly intriguing, since this transcription factor is known to be activated by high concentration of heme which shares with the ergosterol biosynthesis pathway Farnesyl Pyrophosphate (FPP) as precursor (Fig. 6).

Third, there is a significant down-regulation of sugar transporter genes. This could be related to the carbon source regulation which has recently been shown for Cdc53 neddylation [85]. This down-regulation appears to be limited to the RNA level.

Furthermore, the gene ontology analysis of the proteins differentially modulated in *Δcsn5* cells shows a highly significant enrichment of proteins involved in amino acid biosynthesis and metabolism and oxidation-reduction processes. Indeed, genes belonging to these ontology categories were previously found modulated at the mRNA level in other csn mutants from *D. melanogaster*, *A. thaliana* and *Aspergillus nidulans* [57, 73, 98]. Of the five proteins found to have significantly increased levels in the *As. nidulans csnE* mutant (the *Sc*Csn5 orthologue), two (Sam2 and Ilv5) were enzymes involved in aminoacid metabolism [73].

Strikingly, their orthologues in *ScΔcsn5* are down-regulated (Table 3), suggesting that their modulation by CSN is conserved through evolution. The fact that both proteins are not regulated at the RNA level neither in *As. nidulans*, nor in *S. cerevisiae* suggests a direct post transcriptional regulation by the CSN. The mis-regulation of Sam2 and Ilv5 in the *Δcsn5* strain could be responsible for the observed alterations in the expression of several other genes and proteins involved in amino acid biosynthesis and metabolism. In fact, several proteins involved in lysine biosynthesis are also down-regulated in *ScΔcsn5* cells. Among them, we found the homocitrate synthase Lys20, which catalyzes the acetyl CoA-α-chetoglutarate condensation required for lysine biosynthesis. The *A. thaliana* orthologue gene, *IMS2,* is also strongly down-regulated in *csn5*

mutant strain, suggesting that this can be a crucial step in the CSN control on lysine biosynthesis ([69] and Table S2). With regards to genes involved in oxidation-reduction processes there is a striking parallelism in the regulation of the thiol peroxidase and hydroperoxide receptor Hyr1, which is one of the most over-expressed proteins in the *Sc∆csn5* strain (Table 3), and of its *A. thaliana* orthologue *At4g11600* strongly induced in *csn5* mutant ([69] and Table S2). Since this protein is an important sensor of lipid oxidation and is involved in the cellular response to oxidative stress we think that this is a noteworthy feature of CSN regulatory action.

A third protein which is mis-regulated both in *As. nidulans* and in *S. cerevisiae* is 3-hydroxy-3-methyl-glutaryl-CoA (HMG-CoA) synthase (Erg13). Its repression could provide an explanation for the down-regulation of the ergosterol pathway observed in *S. cerevisiae ∆csn5* cells. Indeed, down-regulation of Erg13 could result in a decrease of HMG-CoA synthesis, a crucial step in the isoprenoid biosynthetic pathway (Fig. 6). This is consistent with various observations. The first observation is a reported positive genetic interaction between *CSN5* and *FMS1*, a gene coding for a key enzyme in the pantothenic acid synthesis pathway [100]. The second observation is a general down-regulation of *ACS2* both at RNA and protein level. *ACS2* is one of the two genes coding for the acetyl-CoA synthetase which utilizes acetate to produce acetyl-CoA, the substrate utilized for HMG-CoA synthesis. Indeed, it was recently shown that over-expression of Acs2 leads to a consistent increase in acetyl-CoA and up-regulates seven key-genes in the mevalonate pathway [101].

Similarly, repression of the mevalonate pathway could lead to a reduction in *ACS2* expression. Moreover, this enzyme has a key role in determining the extent of histone acetylation and its regulation could have secondary effects on the *∆csn5* transcriptome [102].

The transcriptional down-regulation of the ergosterol biosynthetic pathway could therefore be the consequence of the decreased availability of HMG-CoA and subsequently of FPP, which is the key precursor in the ergosterol biosynthetic pathway (Fig. 6). Likewise, a decrease in FPP levels could be the cause of a reduction in heme biosynthesis, and therefore of the observed downregulation of

the Hap1 regulon. To this purpose, it should be noted that we observed downregulation both of the aerobic and anaerobic Hap1 targets, which is an effect typically observed in the presence of a reduction in heme biosynthesis under aerobic conditions [88]. Down-regulation both at RNA and protein level of *ERG20* which controls the synthesis of Geranyl-P-P (GPP), the precursor of FPP and of *ERG9*, which controls FPP conversion to squalene on the ergosterol pathway, underscores the relevance of Csn5 control in the isoprenoid biosynthesis (Fig. 6). In yeast as in mammals there is a coordinated regulation of fatty acids and cholesterol [103]. In the *Δcsn5* strain we indeed observed down-regulation of *OLE1* at the RNA level and of *FAS1* at the protein level which are two key-enzymes in the fatty acids biosynthetic pathway. Correspondingly, Chamovitz and co-workers observed misregulation of genes coding for sterol-acyl-transferase and acetyl-CoA acyl-transferase (orthologue of *FAS1*) in *Drosophila csn5* null mutants [57]. It will be interesting in the future to assess if HMG-CoA synthesis can be regulated by CSN also in *Drosophila*, plants and mammals. From this point of view it is noteworthy that in *A. thaliana*, the orthologue of *S. cerevisiae* acyl-CoA reductase (*HMG1/HMG2*) is strongly down-regulated in *csn5* mutants ([69] and Table S2), confirming that the control of mevalonate synthesis, a rate-limiting step in isoprenoid and sterol biosynthesis, by the CSN is indeed conserved through evolution (Fig. 6). It should be noted that in *A. thaliana* the orthologue of the acetyl-CoA carboxilase (*ACC1*) another key-regulator of histone acetylation [102] is up-regulated in *csn5* mutants, confirming that a defect in CSN levels could have important effects in histone modification.

S. cerevisiae is an excellent model organism for studying the regulation of lipid metabolism in eukaryotes, as most of the regulatory mechanisms are conserved between yeast and mammals [103] and chances are that this CSN regulatory role could be conserved also in mammals are likely. Our transcriptomic analysis also points out to a CSN function in regulating, directly or indirectly, Zn metabolism and uptake. The genes coding for the Zn high affinity transporters Zrt1 and Zrt3, as well as the Zn/Fe transporter Fet4 to a lower extent, the Zn transcription factor Zap1, are all down-regulated at the transcript level. As a result, *Δcsn5* cells are sensitive to low Zn, Ni and Cd

concentrations in the medium. It is possible that, similarly to what we suggested for the RP and ergosterol genes, CSN might control the stability of some transcription factors involved in the regulation of the metal transporter genes through the ubiquitin ligase activity. Alternatively, the differential transcription of these genes in the *Δcsn5* might be simply the consequence of the reduced ergosterol content in the membrane. Membranes with lower ergosterol content are known to be more permeable to cations [94]. As a result, Zn, when present at high concentration in the medium, could easily accumulate in the cytoplasm and reduce transport genes expression by negative feedback regulation. The positive regulatory effect of zinc and copper on ergosterol biosynthesis which was recently shown [104] could also be explained by a feedback regulation of divalent cation influx. Indeed, at support of the hypothesis that the Zn-related phenotypes of the *csn5* mutant are due to its lower ergosterol content we show here that also a strain deleted in *ERG6* accumulates zinc in the cytoplasm (Fig. 10). At present we cannot rule out that Zn storage in the vacuole is also defective in the Δ*csn5* strain, and that this can contribute to the increased zinc accumulation in the cytoplasm. Indeed, the *Δcsn5* mutant has a negative genetic interaction with mutants deleted in *ZRC1* [100], which encodes the main Zn importer in the vacuole. Moreover, among the down-regulated proteins in *Δcsn5* (Table 3) we found Vtc4, which is a subunit of the vacuolar transporter chaperone (VTC) complex that is involved in synthesis and transport of polyphosphate to the vacuole [105]. This complex regulates membrane trafficking and Zn storage in the vacuole and deletion of *VTC4* has been previously shown to decrease resistance to zinc [106]. Unbalance in zinc or cadmium uptake have previously shown to cause alterations in free amino acids pools [107] and the expression of some of the proteins which we found significantly down-regulated in *Δcsn5* such as Mae1, Leu1, Bat1, Aro10 and Met6 are directly responding to zinc levels through a complex transcriptional and post-transcriptional regulatory system [101].

Further work will be required in order to establish a defined cause-effect relationship between metal influx deregulation and proteomic alterations in *Δcsn5.*

Taken together, our results suggest that Csn5 has a pervasive effect on budding yeast metabolism. The

effects of Csn5 on yeast metabolism seem to be a hallmark not only of Csn5, but of the whole CSN holocomplex, since a panel of selected genes were found by us to be regulated in a very similar fashion in mutants of four other CSN subunits. It is still not clear, however, whether their regulation is neddylation/deneddylation dependent or independent and additional studies are required. Future studies on a double *Δcsn5/rub1* mutant may help to solve this issue. A recent report [85] indicates that SCF complexes from *csn* mutants in budding yeast fail to release substrate adaptors, which remain bound to the complex even in absence of the substrate and delay the formation of new SCF complexes. A similar scenario could be envisaged for the *csn* mutants from *S. cerevisiae*, where an altered stability of specific transcription factors and of their cognate substrate adaptors, might be responsible for the observed defects. Clearly, further work lays ahead to shed light on this hypothesis.

5. MATERIALS AND METHODS

5.1 Yeast Strains and growth conditions

The yeast strains and plasmid used throughout this work are described in Table 7. All yeast strains were grown in YP medium supplemented with 2% of glucose (YPD). Limiting zinc medium (LZM) was prepared in the same manner as low-iron medium (LIM) [108] except that $ZnSO_4$ in LIM was replaced with 10 µM $FeCl_3$ in LZM. Cell number in liquid cultures was determined by measuring the optical density at 600 nm (OD_{600}). For zinquin staining experiments cells were grown in YDP* (YPD with 1.5 mM triptophane, 80 mM adenine hemisulfate, 0.6 mM methionine, 10 mM succinic acid and 15 mM potassium bicarbonate, Sigma-Aldrich, St. Louis, MO, USA) as described previously [109].

5.2 RNA Extraction

RNA was extracted from 20 mL of *S. cerevisiae* cell cultures at A600 = 1 OD (strains were grown in YPD medium at 30°C). Cells were suspended in 1 mL of AE buffer (50 mM sodium acetate pH 5, 10 mM EDTA (AppliChem GmbH, Darmstadt, Germany) centrifuged and suspended in 0.4 mL of AE buffer plus 1% (w/v) SDS (AppliChem GmbH, Darmstadt, Germany). Cells were lysed with phenol : chloroform (5 : 1 pH 4.7, Sigma-Aldrich), heated at 65 °C for 10 minutes, transferred at −80 °C for 10 min and aqueous phase was separated by centrifugation. After a second extraction with phenol:chloroform (24 : 1, pH 5.2, Sigma-Aldrich), RNA was precipitated with ethanol, dried and suspended in sterile water. RNA quantity and purity were assessed at the Nanodrop ND-1000 spectrophotometer (Thermo Scientific, Waltham, MA, USA), at 260 nm and at 260/230, 260/280 nm ratios, respectively. RNA integrity was assessed by electrophoresis on ethidium bromide stained 1% agarose-formaldehyde gels.

STRAINS	GENOTYPE	SOURCE
W303	*MATa, his3-11, ade2-1, leu2-3,112, ura3-1, trp1-D2, can1-100*	Rothstein (Columbia University)
Δ*csn5*	*MAT*a, *his3-11, ade2-1, leu2-3,112, ura3-1, trp1-D2, can1-100, YDL216C::kanMX4*	This work
Δ*csn9*	*MAT*a, *his3-11, ade2-1, leu2-3,112, ura3-1, trp1-D2, can1-100, YDR179C::kanMX4*	This work
Δ*csn10*	*MAT*a, *his3-11, ade2-1, leu2-3,112, ura3-1, trp1-D2, can1-100, YOL117W::kanMX4*	This work
Δ*csn11*	*MAT*a, *his3-11, ade2-1, leu2-3,112, ura3-1, trp1-D2, can1-100, YIL071C::kanMX4*	This work
Δ*csi1*	*MAT*a, *his3-11, ade2-1, leu2-3,112, ura3-1, trp1-D2, can1-100, YMR025W::kanMX4*	This work
Δ*erg6*	*MAT*a, *his3-11, ade2-1, leu2-3,112, ura3-1, trp1-D2, can1-100, YML008C::kanMX4*	This work

PLASMIDS

p-*CSN5*	PYES2+ *CSN5*, URA3	Open Biosystem
p-*CSN5*	pRS416+ CSN5 promoter-CSN5, URA3	This work
p-*CSN5-(JAMM)*	pYES2+ *CSN5*-(*JAMM*)	[5]

Tab. 7 Strains and plasmids used in this work.

5.3 Microarray analysis

cDNA labeling

20 µg of total RNA extracted from cell culture as described above was mixed with 2 µg of 16mers oligo dT and incubated at 70 °C for 10 min. cDNA was synthesized in a final volume of 40 µl with 25 mM each of dATP, dCTP and dGTP, 15 mM of dTTP, 10 mM of aminoallyl-dUTP, 10 mM DTT and 400 U of SuperScript III reverse transcriptase (Life Technologies, Carlsbad, CA, USA) in 1× reaction buffer.

The samples were incubated for 2 h at 42 °C. RNA was hydrolyzed with 0.1 M NaOH, incubated for 10 min at 70 °C and subsequently neutralized.

cDNA was labeled with Cy3 and HyPer5 Post-Labeling Reactive Dye (GE Healthcare cod. 28-9224-19, Little Chalfont, UK) according to the manufacturer's protocol.

The labeled cDNA was purified using QIAquick® PCR Purification Kit (Qiagen, Venlo, The Netherlands), and eluted with 30µl of double distilled H_2O. The NanoDrop 1000 spectrophotometer was used to quantify Cy3 and HyPer5 incorporation.

Hybridization and image acquisition of microarray

The microarrays used for analysis were the cDNA Microarray Yeast 6.4k ver. 7 purchased from UHN Microarray Centre (Toronto, Canada, http://data.microarrays.ca/arrays/index.htm).

Slides were pre-hybridized at 42 °C for at least 45 min in a solution containing, 5× saline sodium citrate buffer (NaCl/Cit), 0.1% SDS and 0.1% BSA. The labeled cDNAs (Cy3 sample and HyPer5 sample mixed) were added to an equal volume of hybridization buffer containing 50% formamide, 10× NaCl/Cit and 0.2% SDS pre-heated at 70 °C for 3 min.

Hybridization was carried out for 16 h at 42 °C and unbound DNA was washed off using three steps with solutions containing: I. 1X NaCl/Cit, 0.2% SDS pre-heated at 42 °C; II. 0.1X NaCl/Cit, 0.2 % SDS; III. two times 0.1X NaCl/Cit. A PerkinElmer ScanArray Gx Plus Microarray Scanner (PerkinElmer, Waltham, MA, USA) was used to acquire images, and GENEPIX PRO 6.1 software and SCANARRAY EXPRESS software were used to quantify hybridization signals. Absent and marginal spots were flagged automatically by software and subsequently each slide was inspected manually.

Microarray data analysis

We filtered the data to exclude artifacts, saturated spots, and low signal spots. Assuming that most of the genes have unchanged expression, the Cy3/HyPer5 ratios were normalized using Goulphar script [110] (http://transcriptome.ens.fr/goulphar/index.php) running on R software using a Global Lowess Normalization. The parameters used for the hierarchical clustering were the Euclidean distance and the average linkage method.

The data discussed in this publication have been deposited in NCBI's Gene Expression Omnibus [111] and are accessible through GEO Series accession number GSE51563 (http://www.ncbi.nlm.nih.gov/geo/query/acc.cgi?acc=GSE51563).

5.4 Real Time RT-PCR

1 µg of total RNA extracted from cell cultures was reverse transcribed using 200 ng of 16mers oligo dT (Life Technologies) with SuperScript III First-Strand Synthesis System for RT-PCR (Life Technologies), according to the manufacturer' s instructions. cDNA served as template for subsequent real-time PCR reactions that were set up in duplicate for each sample using the SensiMix SYBR Mix (Bioline, London, UK) and an Applied Biosystems Prism 7300 Sequence Detector. The reaction mixtures were kept at 95 °C for 10 min, followed by 40 cycles at 95 °C for 15 s and 60 °C for 1 min. The threshold cycle (Ct) was calculated using the Sequence Detector Systems version 1.2.2 (Life Technologies) by determining the cycle number at which the change in the fluorescence of the reporter dye (ΔRn) crossed the threshold. To synchronize each experiment, the baseline was set automatically by the software. Relative quantification was carried out with the $2^{-\Delta\Delta Ct}$ method [112], using the abundance of Actin transcript as endogenous house-keeping control. Data were statistically analyzed by Student's t-test.

5.5 Label-free Proteomics

Protein extraction

Proteins were extracted from 20 mL of *S. cerevisiae* cell cultures at $A_{600} = 1$ (strains were grown in YPD medium at 30 °C).

The yeast culture was centrifuged at 1200 g for 3 min at 4°C. The cell pellet was washed with 10 mL of 1X Tris buffered saline (NaCl/Tris) (Sigma-Aldrich) and centrifuged as described above. Following centrifugation, the cell pellet was suspended in 500 µL lysis buffer containing 50 mM Tris-HCl (pH 6.8) (Applichem), 1% (w/v) SDS (Applichem), 1% (v/v) 2-mercaptoethanol (Sigma-Aldrich) and protease inhibitor cocktail (2.5 µg mL^{-1} aprotinin, 2.5 µg mL^{-1} chymostatin, 2.5 µg mL^{-1} leupeptin, 0.5 µg mL^{-1} pepstatin A) (Sigma-Aldrich).

The cell were lysed in the presence of 200 µL of glass beads (Sigma-Aldrich) (425–600 µm, acid washed) by vortexing in MultiVortex at 4°C for 30-40 min and centrifuged at 16,000 g for 10 min at 4°C.

The supernatant containing the proteins was collected, drop-frozen in liquid nitrogen and stored at -20° C. Protein concentration of yeast lysate was determined by Bradford assay (Bio-Rad Laboratories, Hercules, CA, USA) using BSA (Sigma-Aldrich) as a standard.

Sample preparation for label-free proteomics

Proteins were digested using the filter-aided sample preparation (FASP) method [113]. Briefly, 65 µg of protein was loaded on the filter, and washed twice with buffer containing 8 M urea. The proteins were then alkylated using iodoacetamide, and the excess reagent was washed through the filters. The reduced and alkylated proteins were digested ON in a wet chamber at 25 °C using endoproteinase LysC, which cleaves at the C terminus of lysine residues, with an enzyme to protein ratio of 1:50. Then trypsin was added with an enzyme to protein ratio of 1 : 100 and digestion was stopped after 4 h. Peptides obtained by FASP were micro strong anion exchange fractionated into six fractions and finally loaded onto C18 StageTips.

Mass spectrometric analysis

LC-MS/MS experiments were performed on a nano-HPLC system Ultimate 3000 connected to an Orbitrap XL Discovery equipped with a nanoelectrospray source (Thermo Fisher Scientific). Each peptide sample was auto-sampled and separated in a 10 cm analytical column (75 µm inner diameter) in-house packed with 3 µm C18 beads (Magic C18AQ 200 Å, Michrom Bioresources, Inc, Auburn, CA, USA) with a 160 minute gradient from 5% to 80% acetonitrile in 0.1% formic acid. The effluent from the HPLC was directly electrosprayed into the mass spectrometer.

The Orbitrap MS instrument was operated in data-dependent mode to automatically switch between

one full-scan MS and five MS/MS acquisitions. Survey full-scan MS spectra (from m/z 300–2000) were acquired in the Orbitrap detector with resolution R = 30,000 at m/z 400. The five most intense peptide ions with charge states ≥ 2 were sequentially isolated with an isolation window of 2 Th to a maximum target value of 500,000 using automatic gain control and fragmented by collision induced dissociation in the linear trap using normalized collision energy of 35 and activation time of 30 ms. Dynamic exclusion was used to minimize the extent of repeat sequencing of the peptides, and singly charged peptides were excluded from sequencing throughout the run.

Standard mass spectrometric conditions for all experiments were: spray voltage, 1.9 kV; no sheath and auxiliary gas flow; heated capillary temperature, 275 °C.

Protein identification

All raw data analysis was performed with MAXQUANT computational proteomics platform (www.maxquant.org) [114] version 1.3.0.5 supported by Andromeda (www.andromeda-search.org) [115] as the database search engine for peptide identifications. Mass tolerance for searches was set to an initial precursor mass window of 6 ppm and a fragment mass window of 0.5 Th. Data were searched with carbamidomethylation as a fixed modification and protein N-terminal acetylation, methionine oxidation and lysine di-glycine modification as variable modifications. A maximum of two mis-cleavages was allowed while protease specificity was set to Trypsin. We used Andromeda to search the data against a concatenated target/decoy (forward and reversed) version of the Yeast ORF database containing 6301 protein entries. The cut-off false discovery rate for proteins and peptides was set to 0.01, and peptides with a minimum of seven amino acids were considered for identification.

Label-free quantification and statistical analysis

Label-free quantification was performed in MAXQUANT. This included quantification of peptides recognized on the basis of mass and retention time but identified in other LC−MS/MS runs (“match between the runs” option in MAXQUANT). Feature-matching between raw files was enabled, using a retention time window of 2 min. MAXQUANT data were filtered for reverse identifications (false positives), contaminants, and “only identified by site”. Only proteins that had a label-free quantification intensity in at least three of the four biological replicates of each strain were included for statistical and clustering analysis.

The data for all the other proteins included in Table 3 are available on request.

Data were evaluated and statistics calculated using the Perseus software (version 1.2, Max Planck Institute of Biochemistry, Martinsried, Germany).

5.6 Saponification and Gas chromatography analysis

Yeast cells were grown to stationary phase at 30˚C. Cells were pelleted in 50 mL conical tubes for 5 min at 5,000 g. Cells were then resuspended in 3 mL alcoholic KOH (25% w/v) and transferred to glass tubes for refluxing at 87˚C for 2 h. After cooling to room temperature and 3 mL of n-heptane and 1 mL sterile H_2O were added to extract the non-saponifiable lipid fraction. Gas chromatography was routinely carried out on an HP5890 series II utilizing a fused silica DB5-MS capillary column (15m x 0.25 mm x 0.25 µm film thickness), with nitrogen as carrier gas using the Hewlett Packard CHEMSTATION software for quantitation [116].

Samples were run in a semi-splitless mode with a starting temperature of 195˚C for 1 min increasing to 240˚C in 20˚C/min increments and then 2˚C/min increments to a final temperature of 280˚C which was held for an additional 5 min.

5.7 Nystatin and Ketokonazole assay

The same amount of the cells (10^4 mL^{-1}) for each sample were spotted in a maxi-well plate with different nistatin and ketokonazole (Sigma-Aldrich) concentrations and incubated at 30°C overnight. Cell number in liquid cultures was determined by measuring the optical density of cell suspensions at 600 nm (A_{600}).

5.8 Zinquin Staining

Yeast strains were grown in YPD* with 500 µM of $ZnSO_4$ and without zinc as control to an optical density of A_{600} = 1. Cells ware pelleted from liquid culture (23°C, 1000×g 1 min). The cells were immediately resuspended and washed for two times with 1 mL of a buffer solution of 50 mM Tris base and 1 mM sodium azide. Cells to be stained were suspended in 50 µl buffer, diluted with a premix of 1 µl of dimethyl sulfoxide and 1 µl of Zinquin ethyl ester (Sigma-Aldrich), mixed gently, and incubated at 23°C for 60 min with occasional mixing. The cells were then washed with buffer, resuspended in three pellet volumes of supernatant, and prepared for microscopy (Zeiss Motorized Axio Imager Z1 Fluorescence Microscope, Zeiss, Oberkochen, Germany). Zinquin stock solutions

were stored at the dark at 23°C.

5.9 LZM experiments

Yeast strains were grown in LZM medium plus different $ZnSO_4$ concentrations (0-600 μM) for16h at 30°C. Cell number in liquid cultures was determined by measuring the optical density of cell suspensions at 600 nm (A_{600}).

6. SUPPLEMENTAL MATERIALS

Table S1 List of selected Δ*csn5/W303* microarray data

Genes which show an average Log2 ratio Δ*csn5/W303* <-0.5 or >0.5 and P-value <0.05 according to Student T-test in the two independent experiments.

Systematic Name	Gene Symbol	Gene Mean	Gene std.dev.	t value	Log2ratio_exp_1	Log2ratio_exp_2
ydr492w	IZH1	-2,701	0,225	16,959	-2,86	-2,54
yhr053c	CUP1-1	-2,672	0,252	14,966	-2,85	-2,49
ydl023c	GPD1	-2,657	0,293	12,821	-2,45	-2,86
yjl144w		-2,408	0,186	18,279	-2,54	-2,28
ygr049w	SCM4	-2,390	0,014	245,105	-2,38	-2,40
yol101c	IZH4	-2,232	0,196	16,143	-2,37	-2,09
yer066c-a	(Not4)	-2,223	0,179	17,540	-2,35	-2,10
yml130c	ERO1	-2,184	0,122	25,395	-2,27	-2,10
ydr342c	HXT7	-2,181	0,072	42,561	-2,13	-2,23
ymr246w	FAA4	-2,091	0,072	41,197	-2,04	-2,14
yhr054c	(Cup1)	-2,044	0,006	454,330	-2,04	-2,05
ykl150w	MCR1	-2,038	0,187	15,408	-2,17	-1,91
ynl142w	MEP2	-1,994	0,047	59,508	-1,96	-2,03
ygr286c	BIO2	-1,993	0,024	119,000	-2,01	-1,98
yil175w		-1,992	0,195	14,463	-2,13	-1,85
yer044c	ERG28	-1,985	0,163	17,221	-2,10	-1,87
ymr182c	RGM1	-1,974	0,037	74,472	-2,00	-1,95
ycl040w	GLK1	-1,944	0,051	53,621	-1,98	-1,91
ypl265w	DIP5	-1,943	0,132	20,839	-1,85	-2,04
ykr039w	GAP1	-1,867	0,038	69,785	-1,84	-1,89
ygl037c	PNC1	-1,847	0,109	23,913	-1,77	-1,92
ykl061w		-1,845	0,007	388,473	-1,85	-1,84
yjr048w	CYC1	-1,842	0,116	22,463	-1,76	-1,92
ymr181c		-1,802	0,111	23,026	-1,88	-1,72
ynr075w	COS10	-1,782	0,124	20,250	-1,87	-1,69
ymr011w	HXT2	-1,756	0,065	37,973	-1,71	-1,80
yel046c	GLY1	-1,696	0,162	14,842	-1,81	-1,58
yhr097c		-1,683	0,179	13,280	-1,81	-1,56
yor052c		-1,664	0,090	26,197	-1,60	-1,73
yhr092c	HXT4	-1,649	0,126	18,528	-1,56	-1,74
ygr036c	CAX4	-1,618	0,152	15,014	-1,51	-1,73
ydr497c	ITR1	-1,537	0,005	472,846	-1,54	-1,53
yal005c	SSA1	-1,533	0,089	24,333	-1,47	-1,60
yjr025c	BNA1	-1,525	0,091	23,636	-1,46	-1,59
ydl049c	KNH1	-1,507	0,032	67,000	-1,53	-1,49
ydr151c	CTH1	-1,507	0,146	14,556	-1,61	-1,40
yol113w	SKM1	-1,506	0,161	13,242	-1,62	-1,39
yll026w	HSP104	-1,483	0,047	44,939	-1,45	-1,52
ydr399w	HPT1	-1,441	0,114	17,842	-1,36	-1,52
ymr202w	ERG2	-1,396	0,094	21,075	-1,33	-1,46
yjr076c	CDC11	-1,388	0,082	24,030	-1,33	-1,45
ybr067c	TIP1	-1,361	0,058	33,393	-1,32	-1,40
yor248w	(srl1)	-1,343	0,060	31,588	-1,30	-1,39
ynl036w	NCE103	-1,338	0,002	764,718	-1,34	-1,34
yar066w		-1,337	0,038	49,518	-1,31	-1,36
yal009w	SPO7	-1,336	0,065	28,892	-1,29	-1,38
ydr074w	TPS2	-1,324	0,136	13,792	-1,42	-1,23
ydl021w	GPM2	-1,310	0,127	14,642	-1,40	-1,22
ygr146c	ECL1	-1,306	0,021	90,034	-1,32	-1,29

ynl052w	COX5A	-1,301	0,028	66,692	-1,32	-1,28
yar073w	IMD1	-1,288	0,081	22,391	-1,23	-1,35
ygl253w	HXK2	-1,287	0,123	14,793	-1,20	-1,37
yclx09w	AGP1	-1,283	0,081	22,304	-1,34	-1,23
yol059w	GPD2	-1,273	0,018	101,800	-1,26	-1,29
ybr289w	SNF5	-1,225	0,064	27,077	-1,18	-1,27
yhr190w	ERG9	-1,208	0,115	14,828	-1,29	-1,13
yel047c		-1,192	0,068	24,969	-1,24	-1,14
ylr225c		-1,192	0,031	54,182	-1,17	-1,21
yclx10c	LEU2	-1,182	0,031	54,333	-1,16	-1,20
ygr204w	ADE3	-1,170	0,128	12,967	-1,08	-1,26
ydr155c	CPR1	-1,161	0,041	40,391	-1,19	-1,13
ypr156c	TPO3	-1,125	0,092	17,308	-1,06	-1,19
ynl255c	GIS2	-1,121	0,070	22,756	-1,17	-1,07
yil009w	FAA3	-1,119	0,016	99,444	-1,13	-1,11
yhr096c	HXT5	-1,114	0,091	17,406	-1,05	-1,18
ydl070w	BDF2	-1,106	0,118	13,209	-1,19	-1,02
ydr296w	MHR1	-1,098	0,032	48,778	-1,12	-1,08
yor247w	SRL1	-1,091	0,055	27,974	-1,13	-1,05
yor298w	MUM3	-1,089	0,098	15,783	-1,02	-1,16
ygr149w		-1,088	0,053	28,815	-1,05	-1,13
ygr249w	MGA1	-1,079	0,097	15,745	-1,01	-1,15
ygl077c	HNM1	-1,075	0,064	23,615	-1,12	-1,03
ynl057w		-1,054	0,062	24,086	-1,01	-1,10
ykl191w	DPH2	-1,039	0,073	20,165	-1,09	-0,99
ykl153w		-1,019	0,100	14,406	-1,09	-0,95
yjl174w	KRE9	-1,019	0,058	24,697	-1,06	-0,98
ygr235c		-1,015	0,007	193,287	-1,02	-1,01
ymr105c	PGM2	-1,015	0,077	18,615	-0,96	-1,07
ypl181w	CTI6	-1,004	0,019	73,000	-0,99	-1,02
yer037w	PHM8	-1,003	0,081	17,596	-1,06	-0,95
ydr188w	CCT6	-0,985	0,077	17,995	-1,04	-0,93
ygr037c	ACB1	-0,976	0,037	37,538	-0,95	-1,00
yhr170w	NMD3	-0,969	0,055	24,846	-0,93	-1,01
ypl032c	SVL3	-0,950	0,099	13,616	-0,88	-1,02
ydr505c	PSP1	-0,948	0,040	33,566	-0,92	-0,98
yil117c	PRM5	-0,938	0,053	24,841	-0,90	-0,98
ybr034c	HMT1	-0,935	0,021	64,448	-0,92	-0,95
ymr205c	PFK2	-0,929	0,100	13,134	-1,00	-0,86
yer038c	KRE29	-0,929	0,002	743,001	-0,93	-0,93
yfl049w	SWP82	-0,925	0,050	26,234	-0,96	-0,89
yfl067w		-0,922	0,045	28,812	-0,89	-0,95
yil053w	RHR2	-0,918	0,068	19,031	-0,87	-0,97
ylr109w	AHP1	-0,913	0,061	21,233	-0,87	-0,96
ygr192c	TDH3	-0,913	0,018	70,231	-0,90	-0,93
yal062w	GDH3	-0,910	0,042	30,831	-0,88	-0,94
yhr103w	SBE22	-0,878	0,031	39,449	-0,90	-0,86
yhr094c	HXT1	-0,878	0,018	70,200	-0,89	-0,87
ykr075c		-0,876	0,006	219,000	-0,88	-0,87
yor062c		-0,870	0,086	14,388	-0,81	-0,93
ydr405w	MRP20	-0,867	0,033	37,696	-0,89	-0,84

ykl056c	TMA19	-0,858	0,068	17,963	-0,81	-0,91
ymr146c	TIF34	-0,858	0,074	16,333	-0,91	-0,81
yjl128c	PBS2	-0,857	0,038	32,028	-0,83	-0,88
ykr093w	PTR2	-0,854	0,034	35,227	-0,83	-0,88
ykr071c	DRE2	-0,850	0,084	14,230	-0,91	-0,79
ymr145c	NDE1	-0,850	0,085	14,167	-0,79	-0,91
ynl144c		-0,850	0,071	17,000	-0,90	-0,80
yjr074w	MOG1	-0,849	0,027	44,117	-0,83	-0,87
ylr347c	KAP95	-0,842	0,040	29,796	-0,87	-0,81
yir016w		-0,841	0,028	43,103	-0,86	-0,82
ycr012w	PGK1	-0,836	0,079	14,929	-0,78	-0,89
ydr071c	PAA1	-0,823	0,052	22,243	-0,86	-0,79
ykr034w	DAL80	-0,813	0,080	14,330	-0,87	-0,76
yjl158c	CIS3	-0,809	0,083	13,712	-0,75	-0,87
ypl044c		-0,808	0,074	15,381	-0,86	-0,76
ykl035w	UGP1	-0,804	0,034	33,500	-0,78	-0,83
ypr032w	SRO7	-0,801	0,087	13,033	-0,74	-0,86
ygr259c		-0,798	0,039	28,748	-0,77	-0,83
yil142w	CCT2	-0,797	0,047	24,152	-0,83	-0,76
yjl090c	DPB11	-0,797	0,024	47,567	-0,78	-0,81
ylr395c	COX8	-0,796	0,021	54,862	-0,81	-0,78
ypl106c	SSE1	-0,793	0,052	21,432	-0,83	-0,76
yjr091c	JSN1	-0,792	0,040	28,027	-0,82	-0,76
ygr087c	PDC6	-0,790	0,000	3158,852	-0,79	-0,79
ybr104w	YMC2	-0,786	0,008	131,000	-0,78	-0,79
ycl050c	APA1	-0,782	0,002	520,996	-0,78	-0,78
yjr086w	STE18	-0,775	0,007	155,000	-0,78	-0,77
yjr046w	TAH11	-0,773	0,010	106,586	-0,78	-0,77
ydl054c	MCH1	-0,767	0,080	13,566	-0,71	-0,82
yer012w	PRE1	-0,758	0,018	60,600	-0,77	-0,75
ylr380w	CSR1	-0,754	0,034	31,103	-0,73	-0,78
ygl224c	SDT1	-0,743	0,032	32,648	-0,72	-0,77
yll019c	KNS1	-0,735	0,049	21,000	-0,77	-0,70
ylr379w		-0,731	0,001	731,009	-0,73	-0,73
ygr135w	PRE9	-0,729	0,055	18,806	-0,69	-0,77
yil036w	CST6	-0,716	0,078	12,892	-0,66	-0,77
ygr254w	ENO1	-0,716	0,050	20,155	-0,68	-0,75
ygl039w		-0,713	0,019	53,830	-0,70	-0,73
ymr244c-a		-0,710	0,071	14,134	-0,66	-0,76
yor157c	PUP1	-0,701	0,015	66,714	-0,69	-0,71
yhl031c	GOS1	-0,689	0,055	17,667	-0,65	-0,73
ymr186w	HSC82	-0,688	0,046	21,154	-0,72	-0,66
ylr099c	ICT1	-0,684	0,034	28,216	-0,66	-0,71
yjl048c	UBX6	-0,681	0,012	77,857	-0,69	-0,67
ydl047w	SIT4	-0,681	0,041	23,274	-0,71	-0,65
ylr101c		-0,677	0,009	104,077	-0,67	-0,68
ynl058c		-0,671	0,072	13,217	-0,62	-0,72
yor375c	GDH1	-0,669	0,040	23,456	-0,64	-0,70
ybr202w	MCM7	-0,668	0,059	16,006	-0,71	-0,63
ypr041w	TIF5	-0,662	0,040	23,643	-0,69	-0,63
ypr139c	VPS66	-0,658	0,011	82,250	-0,65	-0,67

ycl052c	PBN1	-0,653	0,060	15,269	-0,61	-0,70
ypr008w	HAA1	-0,644	0,062	14,636	-0,60	-0,69
yjl162c	JJJ2	-0,642	0,059	15,458	-0,60	-0,68
yjl065c	DLS1	-0,640	0,000	Infinity	-0,64	-0,64
yhr007c	ERG11	-0,637	0,046	19,458	-0,67	-0,60
yhr025w	THR1	-0,629	0,070	12,777	-0,58	-0,68
ydl074c	BRE1	-0,625	0,035	25,000	-0,60	-0,65
ydr072c	IPT1	-0,620	0,042	21,034	-0,65	-0,59
ylr014c	PPR1	-0,620	0,056	15,684	-0,58	-0,66
yhr166c	CDC23	-0,613	0,033	26,652	-0,59	-0,64
ypr028w	YOP1	-0,610	0,042	20,513	-0,64	-0,58
ynl244c	SUI1	-0,605	0,022	39,000	-0,62	-0,59
ygl096w	TOS8	-0,604	0,062	13,727	-0,56	-0,65
ybl028c		-0,596	0,051	16,448	-0,56	-0,63
ydr219c	MFB1	-0,594	0,037	22,396	-0,62	-0,57
ydr354w	TRP4	-0,586	0,023	36,625	-0,57	-0,60
yll064c		-0,583	0,011	77,667	-0,59	-0,58
ymr055c	BUB2	-0,580	0,028	29,000	-0,60	-0,56
yfr050c	PRE4	-0,564	0,062	12,886	-0,52	-0,61
ynl141w	AAH1	-0,561	0,043	18,236	-0,53	-0,59
yor204w	DED1	-0,560	0,029	27,642	-0,58	-0,54
yor344c	TYE7	-0,559	0,027	29,052	-0,54	-0,58
yjr028w		-0,556	0,020	39,000	-0,57	-0,54
ydl133c-a	RPL41B	-0,554	0,051	15,503	-0,59	-0,52
yol115w	PAP2	-0,547	0,004	182,334	-0,55	-0,54
ygr177c	ATF2	-0,546	0,023	33,121	-0,53	-0,56
ymr217w	GUA1	-0,545	0,035	22,030	-0,57	-0,52
ypl179w	PPQ1	-0,544	0,037	20,509	-0,57	-0,52
ybl081w		-0,541	0,016	49,182	-0,53	-0,55
ymr219w	ESC1	-0,534	0,009	82,077	-0,54	-0,53
ydr353w	TRR1	-0,532	0,003	265,999	-0,53	-0,53
ygr046w	TAM41	-0,532	0,059	12,737	-0,49	-0,57
yhl034c	SBP1	-0,527	0,010	78,037	-0,52	-0,53
ygr131w		-0,518	0,012	62,818	-0,51	-0,53
ykl071w		-0,517	0,033	22,478	-0,54	-0,49
ygr175c	ERG1	-0,515	0,015	44,721	-0,47	-0,49
SDH1	-0,513	0,039	18,636	-0,54	-0,49	
ymr009w	ADI1	-0,509	0,041	17,410	-0,48	-0,54
ygl120c	PRP43	-0,491	0,043	16,082	-0,46	-0,52
ymr210w		0,511	0,043	16,738	0,48	0,54
ybr290w	BSD2	0,550	0,056	13,830	0,51	0,59
ylr043c	TRX1	0,550	0,014	56,436	0,56	0,54
ykr001c	VPS1	0,551	0,030	26,238	0,53	0,57
yer186c		0,568	0,011	73,258	0,56	0,58
ylr180w	SAM1	0,569	0,016	51,727	0,58	0,56
ydr086c	SSS1	0,627	0,066	13,473	0,58	0,67
yhr198c		0,640	0,042	21,678	0,61	0,67
ygl242c		0,640	0,071	12,800	0,69	0,59
yjl087c	TRL1	0,646	0,049	18,710	0,68	0,61
ybr149w	ARA1	0,652	0,012	76,647	0,66	0,64
ydl083c	RPS16B	0,657	0,066	14,048	0,61	0,70

yor382w	FIT2	0,659	0,072	12,990	0,71	0,61
ybl070c		0,660	0,057	16,404	0,62	0,70
ypr099c		0,662	0,026	35,757	0,68	0,64
ynl069c	RPL16B	0,675	0,049	19,432	0,71	0,64
yor063w	RPL3	0,691	0,071	13,673	0,64	0,74
ydl005c	MED2	0,692	0,059	16,476	0,65	0,73
yfr033c	QCR6	0,698	0,011	93,000	0,69	0,71
ypr136c		0,709	0,058	17,405	0,75	0,67
ynl023c	FAP1	0,710	0,014	71,000	0,72	0,70
yor264w	DSE3	0,712	0,003	355,999	0,71	0,71
yhr010w	RPL27A	0,716	0,020	51,143	0,73	0,70
ylr334c		0,717	0,024	42,176	0,70	0,73
ybr189w	RPS9B	0,717	0,046	21,901	0,75	0,68
yhl019c	APM2	0,719	0,030	33,824	0,74	0,70
ycr045c		0,719	0,043	23,390	0,75	0,69
yer188w		0,737	0,033	31,688	0,76	0,71
yfl018c	LPD1	0,737	0,032	32,407	0,76	0,71
ykl172w	EBP2	0,750	0,001	1501,019	0,75	0,75
ydl184c	RPL41A	0,763	0,018	58,692	0,75	0,78
yml072c	TCB3	0,765	0,021	51,000	0,78	0,75
ydr046c	BAP3	0,769	0,072	15,078	0,82	0,72
yor321w	PMT3	0,782	0,017	65,167	0,77	0,79
yjl134w	LCB3	0,783	0,010	107,965	0,79	0,78
yor020c	HSP10	0,784	0,051	21,778	0,82	0,75
ygl028c	SCW11	0,819	0,083	13,936	0,76	0,88
ynl309w	STB1	0,819	0,044	26,419	0,85	0,79
ynl013c		0,820	0,028	41,506	0,80	0,84
ybr181c	RPS6B	0,833	0,089	13,222	0,77	0,90
yhl025w	SNF6	0,848	0,045	26,717	0,88	0,82
ylr331c	JIP3	0,849	0,016	73,783	0,86	0,84
ykr061w	KTR2	0,852	0,002	567,674	0,85	0,85
ygr115c		0,857	0,081	15,035	0,80	0,91
yol114c		0,870	0,028	43,500	0,85	0,89
ydl081c	RPP1A	0,895	0,049	25,571	0,93	0,86
ylr390w-a	CCW14	0,896	0,077	16,512	0,95	0,84
yor367w	SCP1	0,902	0,097	13,161	0,97	0,83
ybl027w	RPL19B	0,927	0,066	19,723	0,88	0,97
yjr024c	MDE1	0,927	0,060	21,690	0,97	0,88
ybr031w	RPL4A	0,938	0,025	52,111	0,92	0,96
ygl229c	SAP4	0,943	0,004	342,817	0,94	0,95
ybr280c	SAF1	0,948	0,025	52,667	0,93	0,97
ylr157c	ASP3-2	0,976	0,078	17,577	0,92	1,03
ypr053c		0,985	0,063	22,124	0,94	1,03
ygl104c	VPS73	0,992	0,040	35,106	1,02	0,96
ymr159c	ATG16	0,993	0,052	27,027	1,03	0,96
ymr091c	NPL6	0,996	0,062	22,636	1,04	0,95
ycrx17w		1,019	0,001	1019,013	1,02	1,02
ylr292c	SEC72	1,031	0,058	25,146	0,99	1,07
ylr029c	RPL15A	1,047	0,060	24,497	1,09	1,00
ylr103c	CDC45	1,051	0,101	14,754	0,98	1,12
yll051c	FRE6	1,064	0,090	16,686	1,00	1,13

ymr121c	RPL15B	1,085	0,022	71,131	1,10	1,07
ydl119c		1,097	0,103	15,082	1,17	1,02
yor234c	RPL33B	1,102	0,074	21,192	1,05	1,15
ykr100c	SKG1	1,106	0,005	294,998	1,11	1,10
ykl202w		1,111	0,069	22,673	1,16	1,06
ygr035c		1,118	0,004	447,000	1,12	1,12
ygr083c	GCD2	1,133	0,075	21,282	1,08	1,19
ygl004c	RPN14	1,151	0,084	19,336	1,21	1,09
ylr119w	SRN2	1,159	0,128	12,774	1,25	1,07
ygr078c	PAC10	1,170	0,042	39,644	1,14	1,20
yor315w	SFG1	1,182	0,125	13,350	1,27	1,09
yor355w	GDS1	1,200	0,112	15,088	1,12	1,28
ypl067c		1,211	0,112	15,226	1,29	1,13
yjl006c	CTK2	1,228	0,131	13,270	1,32	1,14
yol083w		1,257	0,067	26,608	1,21	1,30
yhr129c	ARP1	1,259	0,126	14,183	1,17	1,35
yer074w	RPS24A	1,267	0,023	76,758	1,25	1,28
ypl143w	RPL33A	1,272	0,069	26,216	1,32	1,22
yol158c	ENB1	1,294	0,006	304,530	1,29	1,30
ykr040c		1,311	0,044	41,960	1,28	1,34
ypr082c	DIB1	1,328	0,096	19,598	1,26	1,40
yel059w		1,349	0,027	70,091	1,33	1,37
yfr047c	BNA6	1,350	0,086	22,306	1,41	1,29
yil029c		1,358	0,003	678,989	1,36	1,36
yer042w	MXR1	1,366	0,105	18,459	1,44	1,29
ydr485c	VPS72	1,375	0,049	39,841	1,34	1,41
ylr214w	FRE1	1,389	0,129	15,175	1,48	1,30
ykr041w		1,422	0,158	12,749	1,31	1,53
yhr201c	PPX1	1,474	0,080	26,080	1,53	1,42
ygl240w	DOC1	1,497	0,145	14,572	1,60	1,39
ypr043w	RPL43A	1,525	0,092	23,548	1,46	1,59
ydr448w	ADA2	1,566	0,078	28,207	1,51	1,62
yll002w	RTT109	1,567	0,033	66,660	1,59	1,54
yil069c	RPS24B	1,570	0,001	3138,853	1,57	1,57
ynr074c	AIF1	1,576	0,104	21,449	1,65	1,50
ylr226w	BUR2	1,582	0,145	15,474	1,48	1,68
ygl090w	LIF1	1,680	0,184	12,896	1,81	1,55
ydr424c	DYN2	1,684	0,008	280,665	1,69	1,68
ymr085w		1,752	0,026	95,986	1,77	1,73
yjr010w	MET3	1,769	0,183	13,689	1,64	1,90
yol135c	MED7	1,783	0,066	38,144	1,83	1,74
ymr094w	CTF13	1,816	0,019	132,091	1,83	1,80
ykl001c	MET14	1,825	0,007	347,668	1,82	1,83
yor126c	IAH1	1,847	0,075	35,019	1,90	1,79
yjl189w	RPL39	1,863	0,018	143,308	1,85	1,88
ymr031w-a		1,886	0,192	13,915	1,75	2,02
ylr370c	ARC18	1,934	0,009	297,461	1,94	1,93
ylr199c	PBA1	2,021	0,140	20,360	2,12	1,92
ydr278c		2,030	0,028	102,772	2,01	2,05
ylr185w	RPL37A	2,075	0,163	18,007	1,96	2,19
ymr194w	RPL36A	2,184	0,107	28,737	2,26	2,11

ypl081w	RPS9A	2,189	0,030	103,000	2,21	2,17
ygr029w	ERV1	2,225	0,022	145,918	2,21	2,24
ylr078c	BOS1	2,228	0,060	52,412	2,27	2,19
yol137w	BSC6	2,327	0,189	17,427	2,46	2,19
ylr356w		2,347	0,011	312,998	2,34	2,36
ylr377c	FBP1	2,361	0,140	23,911	2,46	2,26
ybr153w	RIB7	2,387	0,103	32,814	2,46	2,31
ylr393w	ATP10	2,405	0,261	13,019	2,59	2,22
ynl179c		2,428	0,187	18,357	2,56	2,30
yml024w	RPS17A	2,538	0,111	32,438	2,46	2,62
yil148w	RPL40A	2,638	0,279	13,354	2,44	2,84
yhr013c	ARD1	2,714	0,118	32,497	2,63	2,80
yor182c	RPS30B	2,731	0,211	18,296	2,88	2,58
yml025c	YML6	2,803	0,193	20,499	2,94	2,67
ylr162w		3,042	0,158	27,278	2,93	3,15
ycl006c		3,163	0,194	23,044	3,30	3,03
yir027c	DAL1	3,241	0,086	53,562	3,18	3,30
yjr038c		3,297	0,288	16,199	3,50	3,09
yer179w	DMC1	4,170	0,155	38,078	4,06	4,28

Table S2 List of modulated genes in specific *A. thaliana csn5* mutant.

List of genes modulated in specific *A. thaliana csn5* mutants grown in the light (L) or the dark (D) (data from [69]). Only genes with correspondent *S. cerevisiae* orthologous are shown (data accessible at NCBI GEO database, accession GSE9728)

1- Arabidopsis Affymetrix ATH1-121501 annotation Probe Set ID

2- Transcript ID(Array Design),

3- UniGene ID

4- Gene Title

5- Ortholog Probe Set

6- Ortholog Target Title

7- Δ*csn5*D_sig.M

8- Δ*csn5*D_sig.adjPVal

9 Δ*csn5*L_sig.M

10 Δ*csn5*L_sig.adjPVal

1	2	3	4	5	6	7	8	9	10
245854_at	At5g13490			1775433_AT	Mitochondrial inner membrane ADP/ATP translocator, exchanges cytosolic ADP for mitochondrially synthesized ATP	1,68	2,16 e^{-06}	1,83	1,54 e^{-06}
246028_at	At5g21170			1776136_AT	One of three beta subunits of the Snf1 serine/threonine protein kinase complex involved in the response to glucose starvation	-2,40	1,34 e^{-06}	-2,85	4,58 e^{-07}
246028_at	At5g21170			1775711_AT	AMP-activated protein kinase beta subunit (predicted)	-2,40	1,34 e^{-06}	-2,85	4,58 e^{-07}
246132_at	At5g20850			1773120_AT	Strand exchange protein, forms a helical filament with DNA that searches for homology	2,62	1,39 e^{-05}	2,27	5,73 e^{-05}
246132_at	At5g20850			1778182_AT	recombinase Rhp51	2,62	1,39 e^{-05}	2,27	5,73 e^{-05}
246290_at	At3g56800			1777026_AT	calmodulin Cam1	-1,33	5,54 e^{-06}	-1,27	1,10 e^{-05}
246463_at	At5g16970	At.22432	At-AER (alkenal reductase)	1779501_AT	NADP-dependent oxidoreductase (predicted)	1,79	8,95 e^{-07}	1,56	3,85 e^{-06}
246559_at	At5g15550	At.27103	---	1770200_AT	Constituent of 66S pre-ribosomal particles, forms a complex with Nop7p and Erb1p that is required for maturation of the large ribosomal subunit	1,44	3,01 e^{-06}	1,52	2,71 e^{-06}
246559_at	At5g15550	At.27103	---	1769680_AT	ribosome biogenesis protein Ytm1 (predicted)	1,44	3,01 e^{-06}	1,52	2,71 e^{-06}
247218_at	At5g65010			1769642_AT	Asparagine synthetase, isozyme of Asn1p	3,68	3,07 e^{-07}	-2,00	5,86 e^{-05}
247218_at	At5g65010			1772615_AT	Asparagine synthetase, isozyme of Asn2p	3,68	3,07 e^{-07}	-2,00	5,86 e^{-05}
247218_at	At5g65010			1778828_AT	Asparagine synthetase	3,68	3,07 e^{-07}	-2,00	5,86 e^{-05}
247362_247218	At5g63140	At.8836	AtPAP29	1776752_AT	Phosphoesterase involved in downregulation of the unfolded protein response, at least in part via dephosphorylation of Ire1p	-1,26	2,57 e^{-05}	-3,77	7,92 e^{-09}
247362_at	At5g63140	At.8836	AtPAP29	1770097_AT	phosphoprotein phosphatase (predicted)	-1,26	2,57 e^{-05}	-3,77	7,92 e^{-09}
247739_at	At5g59240	At.29238	---	1772857_AT	Protein component of the small (40S) ribosomal subunit	1,30	2,21 e^{-05}	1,31	2,65 e^{-05}
247739_at	At5g59240	At.29238	---	1770449_S_AT	Protein component of the small (40S) ribosomal subunit	1,30	2,21 e^{-05}	1,31	2,65 e^{-05}
247739_at	At5g59240	At.29238	---	1770501_AT	Protein component of the small (40S) ribosomal subunit	1,30	2,21 e^{-05}	1,31	2,65 e^{-05}
247739_at	At5g59240	At.29238	---	1772364_AT	40S ribosomal protein S8	1,30	2,21 e^{-05}	1,31	2,65 e^{-05}
247739_at	At5g59240	At.29238	---	1778741_AT	40S ribosomal protein S8	1,30	2,21 e^{-05}	1,31	2,65 e^{-05}
247641_at	At5g60540			1778453_S_AT	Protein of unknown function, nearly identical to Sno2p	1,19	7,01 e^{-05}	1,28	5,02 e^{-05}
247641_at	At5g60540			1772880_AT	Protein of unconfirmed function, involved in pyridoxine metabolism	1,19	7,01 e^{-05}	1,28	5,02 e^{-05}
247641_at	At5g60540			1773786_AT	imidazoleglycerol-phosphate synthase (predicted)	1,19	7,01 e^{-05}	1,28	5,02 e^{-05}
248049_at	At5g56090	At.16897	AtCOX15	1778093_AT	Protein required for the hydroxylation of heme O to form heme A, which is an essential prosthetic group for cytochrome c oxidase	2,53	1,46 e^{-07}	2,79	1,01 e^{-07}
248049_at	At5g56090	At.16897	AtCOX15	1773542_AT	mitochondrial type I [2Fe-2S] ferredoxin Etp1/ cytochrome oxidase cofactor Cox15, fusion	2,53	1,46 e^{-07}	2,79	1,01 e^{-07}
248138_at	At5g54960	At.47515	AtPDC2	1771379_AT	pyruvate decarboxylase (predicted)	2,02	3,96 e^{-05}	1,87	9,40 e^{-05}
248330_at	At5g52810			1772472_AT	ornithine cyclodeaminase family (predicted)	2,51	9,50 e^{-08}	3,15	2,40 e^{-08}

248625_at	At5g48880			1769342_AT	3-ketoacyl-CoA thiolase with broad chain length specificity, cleaves 3-ketoacyl-CoA into acyl-CoA and acetyl-CoA during beta-oxidation of fatty acids	4,41	3,19 e^{-09}	2,55	2,00 e^{-07}
248658_at	At5g48600	At.29839	AtSMC3	1778051_AT	Subunit of the condensin complex	2,31	6,88 e^{-08}	1,72	9,50 e^{-07}
248658_at	At5g48600	At.29839	AtSMC3	1777960_AT	condensin subunit Cut3	2,31	6,88 e^{-08}	1,72	9,50 e^{-07}
248749_at	At5g47880			1771279_AT	Polypeptide release factor (eRF1) in translation termination	2,20	4,47 e^{-05}	3,63	1,04 e^{-06}
248749_at	At5g47880			1774411_AT	translation release factor eRF1	2,20	4,47 e^{-05}	3,63	1,04 e^{-06}
248940_at	At5g45400	At.30014	---	1773412_AT	Subunit of heterotrimeric Replication Protein A (RPA), which is a highly conserved single-stranded DNA binding protein involved in DNA replication, repair, and recombination	2,12	7,82 e^{-07}	1,80	3,93 e^{-06}
248940_at	At5g45400	At.30014	---	1773556_AT	DNA replication factor A subunit Ssb1	2,12	7,82 e^{-07}	1,80	3,93 e^{-06}
248984_at	At5g45140	At.9250	AtNRPC2	1775098_AT	Second-largest subunit of RNA polymerase III, which is responsible for the transcription of tRNA and 5S RNA genes, and other low molecular weight RNAs	1,70	6,65E-06	1,41	4,18E-05
248984_at	At5g45140	At.9250	AtNRPC2	1770301_AT	DNA-directed RNA polymerase III complex subunit Rpc2	1,70	6,65 e^{-06}	1,41	4,18 e^{-05}
249327_at	At5g40890			1770970_AT	ClC chloride channel	-1,80	2,80 e^{-05}	-2,37	3,94 e^{-06}
249658_s_at	At5g36700	At.30537	---	1769961_AT	Alkaline phosphatase specific for p-nitrophenyl phosphate	3,19	4,85 e^{-08}	-1,79	6,55 e^{-06}
249658_s_at	At5g36700	At.30537	---	1772707_AT	4-nitrophenylphosphatase	3,19	4,85 e^{-08}	-1,79	6,55 e^{-06}
249867_at	At5g23020	At.20469	AtIMS2	1771703_AT	Homocitrate synthase isozyme, catalyzes the condensation of acetyl-CoA and alpha-ketoglutarate to form homocitrate, which is the first step in the lysine biosynthesis pathway	-2,74	5,92 e^{-06}	-3,52	1,07 e^{-06}
250197_at	At5g14590	At.46811	---	1772223_AT	Mitochondrial NADP-specific isocitrate dehydrogenase, catalyzes the oxidation of isocitrate to alpha-ketoglutarate	1,26	3,19 e^{-06}	1,50	1,07 e^{-06}
250197_at	At5g14590	At.46811	---	1774828_AT	isocitrate dehydrogenase Idp1	1,26	3,19 e^{-06}	1,50	1,07 e^{-06}
250369_at	At5g11300			1777207_AT	B-type cyclin involved in DNA replication during S phase	2,20	2,17 e^{-06}	1,85	1,21 e^{-05}
250369_at	At5g11300			1777114_AT	B-type cyclin involved in DNA replication during S phase	2,20	2,17 e^{-06}	1,85	1,21 e^{-05}
250733_at	At5g06290			1774211_AT	Thioredoxin peroxidase, acts as both a ribosome-associated and free cytoplasmic antioxidant	1,53	4,31 e^{-05}	-2,09	4,44 e^{-06}
250733_at	At5g06290			1777880_AT	thioredoxin peroxidase Tpx1	1,53	4,31 e^{-05}	-2,09	4,44 e^{-06}
250994_at	At5g02490	At.74798	---	1779158_AT	ATPase involved in protein folding and the response to stress	1,09	8,06 e^{-05}	2,49	1,37 e^{-07}
251020_at	At5g02270			1770376_AT	Part of evolutionarily-conserved CCR4-NOT regulatory complex	2,99	1,14 e^{-06}	3,11	1,12 e^{-06}
251020_at	At5g02270			1771003_AT	CCR4-Not complex subunit Caf16	2,99	1,14 e^{-06}	3,11	1,12 e^{-06}
251298_at	At3g62040	At.24742	---	1773561_AT	Pyrimidine nucleotidase	-3,62	1,73 e^{-08}	-2,69	2,00 e^{-07}
251298_at	At3g62040	At.24742	---	1774333_AT	pyrimidine 5'-nucleotidase (predicted)	-3,62	1,73 e^{-08}	-2,69	2,00 e^{-07}
251499_at	At3g59100	At.53996	AtGSL11	1772521_AT	Catalytic subunit of 1,3-beta-D-glucan synthase, functionally redundant with alternate catalytic subunit Gsc2p	2,00	5,07 e^{-06}	2,26	2,64 e^{-06}
251499_at	At3g59100	At.53996	AtGSL11	1773780_AT	Catalytic subunit of 1,3-beta-glucan synthase, involved in formation of the inner layer of the spore wall	2,00	5,07 e^{-06}	2,26	2,64 e^{-06}

251499_at	At3g59100	At.53996	ATGSL11	1770805_AT	1,3-beta-glucan synthase subunit Bgs2	2,00	5,07 e^{-06}	2,26	2,64E-06
251499_at	At3g59100	At.53996	AtGSL11	1773407_AT	1,3-beta-glucan synthase subunit Bgs4	2,00	5,07 e^{-06}	2,26	2,64 e^{-06}
251593_at	At3g57660	At.50286	AtNRPA1	1770824_AT	RNA polymerase I largest subunit A190	1,71	6,54 e^{-06}	1,42	3,84 e^{-05}
251593_at	At3g57660	At.50286	AtNRPA1	1772557_AT	DNA-directed RNA polymerase I complex large subunit Nuc1	1,71	6,54 e^{-06}	1,42	3,84 e^{-05}
251678_at	At3g56990	At.28199	AtEDA7	1773994_AT	Essential nucleolar protein, required for biogenesis of the small ribosomal subunit	1,10	3,65 e^{-05}	1,10	5,02 e^{-05}
251678_at	At3g56990	At.28199	AtEDA7	1772492_AT	rRNA processing protein Enp2 (predicted)	1,10	3,65 e^{-05}	1,10	5,02 e^{-05}
251680_at	At3g57060	At.53962	---	1779459_AT	Subunit of the condensin complex	1,87	1,60 e^{-06}	1,54	1,08 e^{-05}
251680_at	At3g57060	At.53962	---	1774278_AT	condensin, non-SMC subunit Cnd1	1,87	1,60 e^{-06}	1,54	1,08 e^{-05}
251740_at	At3g56070	At.34965	AtROC2	1773181_AT	Mitochondrial peptidyl-prolyl cis-trans isomerase (cyclophilin), catalyzes the cis-trans isomerization of peptide bonds N-terminal to proline residues	1,45	1,30 e^{-06}	1,32	3,93 e^{-06}
251846_at	At3g54560			1776021_AT	Histone variant H2AZ, exchanged for histone H2A in nucleosomes by the SWR1 complex	2,20	2,34 e^{-08}	1,17	4,53 e^{-06}
251846_at	At3g54560			1771144_AT	histone H2A variant Pht1	2,20	2,34 e^{-08}	1,17	4,53 e^{-06}
251920_at	At3g53900			1773216_AT	uracil phosphoribosyltransferase (predicted)	2,19	1,27 e^{-07}	-1,15	3,14 e^{-05}
252962_at	At4g38780	At.31150	---	1777272_AT	Component of the U4/U6-U5 snRNP complex, involved in the second catalytic step of splicing	1,48	6,98 e^{-06}	2,20	3,69 e^{-07}
252962_at	At4g38780	At.31150	---	1778236_AT	U5 snRNP complex subunit Spp42	1,48	6,98 e^{-06}	2,20	3,69 e^{-07}
252968_at	At4g38890	At.31136	---	1769388_AT	Dihydrouridine synthase, member of a widespread family of conserved proteins including Smm1p, Dus1p, and Dus4p	1,56	4,81 e^{-07}	1,33	2,51 e^{-06}
252968_at	At4g38890	At.31136	---	1776110_AT	tRNA dihydrouridine synthase Dus3 (predicted)	1,56	4,81 e^{-07}	1,33	2,51 e^{-06}
253013_at	At4g37910	At.2734	AtmtHsc70-1	1771794_AT	Heat shock protein of the Hsp70 family, localized in mitochondrial nucleoids, plays a role in protein translocation, interacts with Mge1p in an ATP-dependent manner	1,84	5,22 e^{-07}	1,68	1,49 e^{-06}
253733_at	At4g29170	At.31952	AtMND1	1777615_AT	meiosis specific coiled-coil protein Mcp7	2,38	2,19 e^{-05}	2,76	8,60 e^{-06}
255310_at	At4g04955			1774012_AT	Allantoinase, converts allantoin to allantoate in the first step of allantoin degradation	-1,95	5,81 e^{-06}	-2,27	2,29 e^{-06}
254890_at	At4g11600			1772259_AT	Thiol peroxidase that functions as a hydroperoxide receptor to sense intracellular hydroperoxide levels and transduce a redox signal to the Yap1p transcription factor	1,17	1,42 e^{-05}	1,93	3,07 e^{-07}
254890_at	At4g11600			1779273_AT	glutathione peroxidase Gpx1	1,17	1,42 e^{-05}	1,93	3,07 e^{-07}
254918_at	At4g11260			1777663_AT	Cochaperone protein	-2,80	5,20 e^{-06}	-2,70	9,49 e^{-06}
254918_at	At4g11260			1773762_AT	SGT1-like protein Git7	-2,80	5,20 e^{-06}	-2,70	9,49 e^{-06}
255011_at	At4g10040			1774137_AT	Cytochrome c isoform 2, expressed under hypoxic conditions	2,41	2,67 e^{-07}	2,81	1,15 e^{-07}
255065_s_at	At4g08870			1779474_AT	agmatinase 2 (predicted)	2,52	6,45 e^{-06}	1,86	9,86 e^{-05}
255225_at	At4g05410	At.33853	---	1778323_AT	Protein involved in pre-rRNA processing, associated with U3 snRNP	1,33	3,65 e^{-05}	1,22	9,43 e^{-05}
255225_at	At4g05410	At.33853	---	1775200_AT	U3 snoRNP-associated protein Rrp9 (predicted)	1,33	3,65 e^{-05}	1,22	9,43 e^{-05}
256459_at	At1g36180	At.51973	AtACC2	1772882_AT	Acetyl-CoA carboxylase, biotin containing enzyme that catalyzes the carboxylation of acetyl-CoA to form malonyl-CoA	2,80	1,76 e^{-05}	2,50	5,90 e^{-05}
256459_at	At1g36180	At.51973	AtACC2	1772858_AT	acetyl-CoA/biotin carboxylase	2,80	1,76 e^{-05}	2,50	5,90 e^{-05}

256852_at	At3g18610	At.5375	AtRANGAP1	1772817_AT	Nucleolar protein that binds nuclear localization sequences, required for pre-rRNA processing and ribosome biogenesis	1,27	2,37 e^{-05}	1,97	8,87 e^{-07}
256852_at	At3g18610	At.5375	AtRANG	1771110_AT	nucleolar protein required for rRNA processing	1,27	2,37 e^{-05}	1,97	8,87 e^{-07}
257148_at	At3g27240			1776968_AT	Cytochrome c1, component of the mitochondrial respiratory chain	1,69	6,97 e^{-07}	1,33	6,74 e^{-06}
257148_at	At3g27240			1772758_AT	cytochrome c1 Cyt1 (predicted)	1,69	6,97 e^{-07}	1,33	6,74 e^{-06}
257149_at	At3g27280			1778425_AT	Subunit of the prohibitin complex (Phb1p-Phb2p), a 1.2 MDa ring-shaped inner mitochondrial membrane chaperone that stabilizes newly synthesized proteins	1,42	3,76 e^{-06}	1,27	1,19 e^{-05}
257149_at	At3g27280			1778529_AT	prohibitin Phb1	1,42	3,76 e^{-06}	1,27	1,19 e^{-05}
257185_at	At3g13100			1779445_AT	Vacuolar glutathione S-conjugate transporter	1,08	7,54 e^{-05}	2,41	1,56 e^{-07}
257185_at	At3g13100			1771947_AT	ABC transporter Abc3	1,08	7,54 e^{-05}	2,41	1,56 e^{-07}
257185_at	At3g13100			1777165_AT	glutathione S-conjugate-exporting ATPase Abc2	1,08	7,54 e^{-05}	2,41	1,56 e^{-07}
257652_at	At3g16810			1771126_AT	Pumilio-homology domain protein that binds the 3' UTR of ASH1 mRNA and represses its translation, resulting in proper asymmetric localization of ASH1 mRNA	1,27	1,71 e^{-05}	1,51	5,91 e^{-06}
257652_at	At3g16810			1773155_AT	Puf family RNA-binding protein	1,27	1,71 e^{-05}	1,51	5,91 e^{-06}
257749_at	At3g18780			1769719_AT	Actin, structural protein involved in cell polarization, endocytosis, and other cytoskeletal functions	-1,65	8,95 e^{-07}	-1,28	9,61 e^{-06}
257749_at	At3g18780			1769830_AT	actin Act1	-1,65	8,95 e^{-07}	-1,28	9,61 e^{-06}
257813_at	At3g25100	At.4990	AtCDC45	1771269_AT	DNA replication initiation factor	2,82	1,08 e^{-06}	2,58	2,99 e^{-06}
257813_at	At3g25100	At.4990	AtCDC45	1776060_AT	DNA replication pre-initiation complex subunit Cdc45	2,82	1,08 e^{-06}	2,58	2,99 e^{-06}
258054_at	At3g16240			1780248_AT	Spore-specific water channel that mediates the transport of water across cell membranes, developmentally controlled	-2,83	7,15 e^{-07}	-4,31	3,77 e^{-08}
258316_at	At3g22660	At.6297	---	1772847_AT	Required for 25S rRNA maturation and 60S ribosomal subunit assembly	1,47	2,33 e^{-05}	1,72	8,44 e^{-06}
258316_at	At3g22660	At.6297	---	1771656_AT	rRNA processing protein Ebp2	1,47	2,33 e^{-05}	1,72	8,44 e^{-06}
258380_at	At3g16650			1771433_AT	Member of the NineTeen Complex (NTC) that contains Prp19p and stabilizes U6 snRNA in catalytic forms of the spliceosome containing U2, U5, and U6 snRNAs	1,42	2,63 e^{-06}	2,07	1,77 e^{-07}
258380_at	At3g16650			1775434_AT	WD repeat protein Prp5	1,42	2,63 e^{-06}	2,07	1,77 e^{-07}
258505_at	At3g06530	At.46312	---	1770861_AT	Nucleolar protein, component of the small subunit (SSU) processome containing the U3 snoRNA that is involved in processing of pre-18S rRNA	1,33	1,89 e^{-05}	1,24	4,36 e^{-05}
258505_at	At3g06530	At.46312	---	1769401_AT	U3 snoRNP-associated protein Utp10 (predicted)	1,33	1,89 e^{-05}	1,24	4,36 e^{-05}
258637_at	At3g07880			1776814_AT	Rho GDP dissociation inhibitor involved in the localization and regulation of Cdc42p and Rho1p	-1,37	8,22 e^{-07}	-1,41	8,84 e^{-07}
258637_at	At3g07880			1771431_AT	Rho GDP dissociation inhibitor Rdi1 (predicted)	-1,37	8,22 e^{-07}	-1,41	8,84 e^{-07}
260211_at	At1g74440	At.4150	---	1780113_AT	DUF962 family protein	1,99	2,48 e^{-05}	1,94	4,11 e^{-05}
259069_at	At3g11710			1779238_AT	Lysyl-tRNA synthetase	1,87	1,23 e^{-07}	1,40	1,80 e^{-06}
259069_at	At3g11710			1770264_AT	cytoplasmic lysine-tRNA ligase Krs1 (predicted)	1,87	1,23 e^{-07}	1,40	1,80 e^{-06}

259475_at	At1g19140			1779932_AT	Protein required for ubiquinone (coenzyme Q) biosynthesis and respiratory growth	2,84	1,54 e^{-08}	1,68	1,09 e^{-06}
259475_at	At1g19140			1774414_AT	ubiquinone biosynthesis protein Coq9 (predicted)	2,84	1,54 e^{-08}	1,68	1,09 e^{-06}
259908_at	At1g60850			1773288_AT	RNA polymerase subunit AC40, common to RNA polymerase I and III	1,23	2,97 e^{-05}	1,15	6,65 e^{-05}
259908_at	At1g60850			1778900_AT	DNA-directed RNA polymerase I and III subunit Rpc40 (predicted)	1,23	2,97 e^{-05}	1,15	6,65 e^{-05}
259983_at	At1g76490			1771313_AT	One of two isozymes of HMG-CoA reductase that catalyzes the conversion of HMG-CoA to mevalonate, which is a rate-limiting step in sterol biosynthesis	-2,28	1,55 e^{-06}	-1,77	1,67 e^{-05}
259983_at	At1g76490			1779769_AT	One of two isozymes of HMG-CoA reductase that convert HMG-CoA to mevalonate, a rate-limiting step in sterol biosynthesis	-2,28	1,55 e^{-06}	-1,77	1,67 e^{-05}
259983_at	At1g76490			1770918_AT	3-hydroxy-3-methylglutaryl-CoA reductase Hmg1	-2,28	1,55 e^{-06}	-1,77	1,67 e^{-05}
260294_at	At1g63660	At.6717	---	1779734_AT	GMP synthase	1,88	3,07 e^{-07}	1,31	7,81 e^{-06}
260294_at	At1g63660	At.6717	---	1779651_AT	GMP synthase [glutamine-hydrolyzing] (predicted)	1,88	3,07 e^{-07}	1,31	7,81 e^{-06}
260704_at	At1g32470			1770632_AT	H subunit of the mitochondrial glycine decarboxylase complex, required for the catabolism of glycine to 5,10-methylene-THF	1,53	3,24 e^{-05}	-1,83	1,00 e^{-05}
260704_at	At1g32470			1771647_AT	glycine decarboxylase complex subunit H	1,53	3,24 e^{-05}	-1,83	1,00 e^{-05}
261064_at	At1g07510	At.23339	AtFTSH10	1773134_AT	Component, with Afg3p, of the mitochondrial inner membrane m-AAA protease that mediates degradation of misfolded or unassembled proteins and is also required for correct assembly of mitochondrial enzyme complexes	1,58	2,75 e^{-06}	1,36	1,24 e^{-05}
261064_at	At1g07510	At.23339	AtFTSH10	1769762_AT	mitochondrial m-AAA protease	1,58	2,75 e^{-06}	1,36	1,24 e^{-05}
261122_at	At1g75330			1770352_AT	Ornithine carbamoyltransferase (carbamoylphosphate:L-ornithine carbamoyltransferase), catalyzes the sixth step in the biosynthesis of the arginine precursor ornithine	1,51	1,20 e^{-06}	1,06	2,88 e^{-05}
261122_at	At1g75330			1771421_AT	ornithine carbamoyltransferase Arg3	1,51	1,20 e^{-06}	1,06	2,88 e^{-05}
261513_at	At1g71840			1778083_AT	ribosome biogenesis protein Sqt1 (predicted)	1,07	3,68 e^{-05}	1,02	6,90 e^{-05}
261664_s_at	At1g18320	At.41800	---	1773950_AT	TIM22 inner membrane protein import complex subunit Tim22	1,45	7,26 e^{-06}	1,45	9,98 e^{-06}
262036_at	At1g35530	At.39558	---	1776741_AT	ATP-dependent 3' to 5' DNA helicase (predicted)	1,71	3,38 e^{-06}	2,59	1,65 e^{-07}
262963_at	At1g54220			1776215_AT	Dihydrolipoamide acetyltransferase component (E2) of pyruvate dehydrogenase complex, which catalyzes the oxidative decarboxylation of pyruvate to acetyl-CoA	1,95	7,41E-07	1,27	3,16E-05
262963_at	At1g54220			1774510_AT	dihydrolipoamide S-acetyltransferase E2 (predicted)	1,95	7,41 e^{-07}	1,27	3,16 e^{-05}
262412_at	At1g34760			1769605_AT	14-3-3 protein Rad24	-3,78	2,79 e^{-07}	-1,96	7,62 e^{-05}
262584_at	At1g15440	At.28488	---	1771819_AT	Conserved 90S pre-ribosomal component essential for proper endonucleolytic cleavage of the 35 S rRNA precursor at A0, A1, and A2 sites	1,87	9,13 e^{-07}	1,58	4,77 e^{-06}
262584_at	At1g15440	At.28488	---	1773526_AT	U3 snoRNP-associated protein Utp1	1,87	9,13 e^{-07}	1,58	4,77 e^{-06}
263824_at	At2g40360	At.25164	---	1769597_AT	Constituent of 66S pre-ribosomal particles, forms a complex with Nop7p and Ytm1p that is required for maturation of the large ribosomal subunit	1,37	1,78 e^{-05}	1,42	1,77 e^{-05}
263824_at	At2g40360	At.25164	---	1776313_AT	WD repeat/BOP1NT protein	1,37	1,78 e^{-05}	1,42	1,77 e^{-05}

263882_at	At2g21790			1778919_AT	Major isoform of the large subunit of ribonucleotide-diphosphate reductase	3,12	2,31 e^{-08}	2,68	1,04 e^{-07}
263882_at	At2g21790			1780044_AT	Minor isoform of the large subunit of ribonucleotide-diphosphate reductase	3,12	2,31 e^{-08}	2,68	1,04 e^{-07}
263882_at	At2g21790			1772861_AT	ribonucleoside reductase large subunit Cdc22	3,12	2,31 e^{-08}	2,68	1,04 e^{-07}
264209_at	At1g22740			1779909_AT	GTPase Ypt71	-3,05	3,31 e^{-08}	-3,25	2,87E-08
264482_at	At1g77210	At.10767	---	1774000_S_AT	Protein of unknown function with similarity to hexose transporter family members, expression is repressed by high levels of glucose	-2,97	1,54 e^{-08}	-1,91	5,31 e^{-07}
264482_at	At1g77210	At.10767	---	1775868_S_AT	Hexose transporter, induced in the presence of non-fermentable carbon sources, induced by low levels of glucose, repressed by high levels of glucose	-2,97	1,54 e^{-08}	-1,91	5,31 e^{-07}
264482_at	At1g77210	At.10767	---	1775358_AT	Hexose transporter, induced in the presence of non-fermentable carbon sources, induced by low levels of glucose, repressed by high levels of glucose	-2,97	1,54 e^{-08}	-1,91	5,31 e^{-07}
264482_at	At1g77210	At.10767	---	1771165_X_AT	Hexose transporter, induced in the presence of non-fermentable carbon sources, induced by low levels of glucose, repressed by high levels of glucose	-2,97	1,54 e^{-08}	-1,91	5,31 e^{-07}
264482_at	At1g77210	At.10767	---	1770625_X_AT	Hexose transporter, up-regulated in media containing raffinose and galactose at pH 7.7 versus pH 4.7, repressed by high levels of glucose	-2,97	1,54 e^{-08}	-1,91	5,31 e^{-07}
265329_at	At2g18450	At.39995	AtSDH1-2	1772202_AT	Flavoprotein subunit of succinate dehydrogenase (Sdh1p, Sdh2p, Sdh3p, Sdh4p), which couples the oxidation of succinate to the transfer of electrons to ubiquinone as part of the TCA cycle and the mitochondrial respiratory chain	2,61	6,17 e^{-08}	1,46	8,46 e^{-06}
265329_at	At2g18450	At.39995	AtSDH1-2	1779916_AT	succinate dehydrogenase Sdh1	2,61	6,17 e^{-08}	1,46	8,46 e^{-06}
265926_at	At2g18600	At.39967	---	1769896_AT	NEDD8-conjugating enzyme Ubc12	2,58	3,98 e^{-06}	2,95	1,87 e^{-06}
267118_at	At2g32590	At.53004	---	1772894_AT	Subunit of the condensin complex	3,26	1,66 e^{-07}	2,42	2,49 e^{-06}
267118_at	At2g32590	At.53004	---	1774405_AT	condensin, non-SMC subunit Cnd2	3,26	1,66 e^{-07}	2,42	2,49 e^{-06}
267454_at	At2g33730	At.27506	---	1778310_AT	U5 snRNP-associated protein Prp28 (predicted)	1,49	5,35 e^{-07}	1,51	6,51 e^{-07}
267492_at	At2g30620			1769850_AT	Histone H1, a linker histone required for nucleosome packaging at restricted sites	-1,13	2,05 e^{-05}	-1,79	6,50 e^{-07}
267627_at	At2g42270	At.43726	---	1770228_AT	RNA-dependent ATPase RNA helicase (DEIH box)	1,31	7,76 e^{-05}	1,54	2,92 e^{-05}
267627_at	At2g42270	At.43726	---	1777512_AT	U5 snRNP complex subunit Brr2 (predicted)	1,31	7,76 e^{-05}	1,54	2,92 e^{-05}

7. REFERENCES

1- Wei N, Serino G & Deng XW (2008) The COP9 signalosome: more than a protease. *Trends Biochem. Sci.* **33**, 592–600.

2- Chamovitz DA, Wei N, Osterlund MT, von Arnim AG, Staub JM, Matsui M & Deng XW (1996) The COP9 complex, a novel multisubunit nuclear regulator involved in light control of a plant developmental switch. *Cell* **86**, 115-121.

3- Wei N, Chamovitz DA & Deng XW (1994) Arabidopsis COP9 is a component of a novel signaling complex mediating light control of development. *Cell* **78**, 117-124.

4- Cope GA, Suh GS, Aravind L, Schwarz SE, Zipursky SL, Koonin EV & Deshaies RJ (2002) Role of predicted metalloprotease motif of Jab1/Csn5 in cleavage of Nedd8 from Cul1. *Science* **298**, 608-611

5- Harari-Steinberg O & Chamovitz DA (2004) The Cop9 signalosome mediating between kinase signaling and protein degradation. *Curr. Protein Pept. Sci.* **5**, 185-189

6- Schwechheimer C & Deng XW (2001) Cop9 signalosome revisited: a novel mediator of protein degradation. *Trends Cell. Biol.* **11**, 420-426

7- von Arnim AG (2003) On again-off again: Cop9 signalosome turns the key of protein degradation. *Curr. Opin. Plant Biol*. **6**, 520-529

8- Wolf DA, Zhou C & Wee S (2003) The Cop9 signalosome: an assembly and maintenance platform for cullin ubiquitin ligases? *Nat. Cell Biol.* **8**, 919-1033

9- Aravind L & Ponting CP (1998) Homologues of 26S proteasome subunits are regulators of transcription and translation. *Protein Sci* **7**, 1250-1254

10- Glickman MH, Rubin DM, Coux O, Wefes I, Pfeifer G, Cjeka Z, Baumeister W, Fried VA & Finley D (1998) A subcomplex of the proteasome regulatory particle required for ubiquitin-conjugate degradation and related to the COP9-signalosome and eIF3. *Cell* **94**, 615-623.

11- Hofmann K & Bucher P (1998) The PCI domain: a common theme in three multiprotein complexes. *Trends Biochem Sci* **23**, 204-205.

12- Petroski MD & Deshaies RJ (2005) Function and regulation of cullin-RING ubiquitin ligases. *Nat. Rev. Mol. Cell Biol.* **6**, 9-20.

13- Lyapina S, Cope G, Shevchenko A, Serino G, Tsuge T, Zhou C, Wolf DA, Wei N, Shevchenko A & Deshaies RJ (2001) Promotion of NEDD-CUL1 conjugate cleavage by COP9 signalosome. *Science* **292**, 1382–1385.

14- Emberley ED, Mosadeghi R & Deshaies RJ (2012) Deconjugation of Nedd8 from Cul1 is directly regulated by Skp1-F-box and substrate, and the COP9 signalosome inhibits deneddylated SCF by a noncatalytic mechanism. *J. Biol. Chem.* **287**, 29679–29689.

15- Serino G & Pick E (2013) Duplication and familial promiscuity within the proteasome lid and COP9 signalosome kin complexes. *Plant Sci. Int. J. Exp. Plant Biol.* **203-204**, 89–97.

16- Ambroggio XI, Rees DC & Deshaies RJ (2004) JAMM: a metalloprotease-like zinc site in the proteasome and signalosome. *Plos Biol.* **2**, E2

17- Duda DM, Borg LA, Scott DC, Hunt HW, Hammel M & Schulman BA (2008) Structural insights into NEDD8 activation of cullin-RING ligases: conformational control of conjugation. *Cell* **134**, 995–1006.

18- Kawakami T, Chiba T, Suzuki T, Iwai K, Yamanaka K, Minato N, Suzuki H, Shimbara N, Hidaka Y, Osaka F, Omata M & Tanaka K (2001) NEDD8 recruits E2-ubiquitin to SCF E3 ligase. *Embo J.* **20**, 4003–4012.

19- Read MA, Brownell JE, Gladysheva TB, Hottelet M, Parent LA, Coggins MB, Pierce JW, Podust VN, Luo RS, Chau V & Palombella VJ (2000) Nedd8 modification of cul-1 activates SCF(beta(TrCP))-dependent ubiquitination of IkBa. *Mol. Cell. Biol.* **20**, 2326–2333.

20- Saha A & Deshaies RJ (2008) Multimodal activation of the ubiquitin ligase SCF by Nedd8 conjugation. *Mol. Cell* **32**, 21–31.

21- Cope GA & Deshaies RJ (2006) Targeted silencing of Jab1/Csn5 in human cells downregulates SCF activity through reduction of F-box protein levels. *Bmc Biochem.* **7**, 1.

22- Denti S, Fernandez-Sanchez ME, Rogge L & Bianchi E (2006) The COP9 signalosome regulates Skp2 levels and proliferation of human cells. *J. Biol. Chem.* **281**, 32188–32196.

23- Wee S, Geyer RK, Toda T & Wolf DA (2005) CSN facilitates Cullin-RING ubiquitin ligase function by counteracting autocatalytic adapter instability. *Nat. Cell Biol.* **7**, 387–391.

24- Enchev RI, Scott DC, da Fonseca PCA, Schreiber A, Monda JK, Schulman BA, Peter M &

Morris EP (2012) Structural basis for a reciprocal regulation between SCF and CSN. *Cell Reports* **2**, 616–627.

25- Fischer ES, Scrima A, Böhm K, Matsumoto S, Lingaraju GM, Faty M, Yasuda T, Cavadini S, Wakasugi M, Hanaoka F, Iwai S, Gut H, Sugasawa K & Thomä NH (2011) The molecular basis of CRL4DDB2/CSA ubiquitin ligase architecture, targeting, and activation. *Cell* **147**, 1024–1039.

26- Zhou Z, Wang Y, Cai G & He Q (2012) Neurospora COP9 signalosome integrity plays major roles for hyphal growth, conidial development, and circadian function. *Plos Genet.* **8**, e1002712.

27- Wang B, Hurov K, Hofmann K & Elledge S. (2009) NBA1, a new player in the Brca1 A complex, is required for DNA damage resistance and checkpoint control. *Genes Dev* **23**, 729-739.

28- Dessau M, Halimi Y, Erez T, Chomsky-Hecht O, Chamovitz DA & Hirsch JA (2008) The Arabidopsis Cop9 signalosome subunit 7 is a model PCI domain protein with a subdomain involved in Cop9 signalosome assembly. *Plant Cell* **20**, 2815-2834.

29- Sharon M, Mao H, Boeri Erba E, Stephens E, Zheng N & Robinson CV (2009) Symmetrical modularity of the Cop9 signalosome complex suggests its multifunctionality. *Structure* **17**, 31-40.

30- Chang EC & Schwechheimer C (2004) ZOME III: the interface between signalling and proteolysis. Meeting on the Cop9 signalosome, Proteasome and eIF3. *EMBO Rep*. **5**, 1041-1045.

31- Pick E & Pintard L (2009) A journey to the land of the rising sun with the Cop9/signalosome and related Zomes. *EMBO Rep*. **4**, 343-348

32- von Arnim AG & Schwechheimer C. (2006) Life is degrading-thanks to some zomes. *Mol Cell.* **23**, 621-629

33- Scheel H & Hofmaan K (2005) Prediction of a common structural scaffold for proteasome lid, Cop9 signalosome and eIF3 complexes. *BMC Bioinformatics* **6**,71

34- Lander GC, Estrin E, Matyskiela ME, Bashore C, Nogales E & Martin A (2012) Complete subunit architecture of the proteasome regulatory particle. *Nature* **482**, 186-191

35- Tsuge T, Matsui M & Wei N (2001) The subunit 1 of the Cop9 signalosome suppresse gene expression through its N-terminal domain and incorporates into the complex through the PCI domain. *J. Mol. Biol.* **305**, 1-9

36- Chamovitz DA (2009) Revisiting the COP9 signalosome as a transcriptional regulator. *EMBO Rep.* **10**, 352-358.

37- Chamovitz DA & Segal D (2001) JAB1/CSN5 and the Cop9 signalosome. A complex situation. *EMBO Rep*. **2**, 96-101.

38- Tomoda K, Kubota Y, Arata Y, Mori S, Maeda M, Tanaka T, Yoshida M, Yoneda-Kato N & Kato JY (2002) The citoplasmic shuttling and subsequent degradation of p27Kip1 mediated by Jab1/Csn5 and the Cop9 signalosome complex. *J.Biol. Chem.* **227**, 2302-2310.

39- Wei N & Deng XW (2003) The Cop9 signalosome. *Annu. Rev. Cell. Dev. Biol*. **19**, 261-286.

40- Zhang H, Gao ZQ, Wang WJ, Liu GF, Shtykova EV, Xu JH, Li LF, Su XD & Dong YH (2012) The crystal structure of the MPN domain from the COP9 signalosome subunit CSN6. *FEBS Lett.* **586**,1147-53.

41- Echalier A, Pan Y, Birol M, Tavernier N, Pintard L, Hoh F, Ebel C, Galophe N, Claret FX & Dumas C (2013) Insights into the regulation of the human COP9 signalosome catalytic subunit, CSN5/Jab1. *Proc. Natl. Acad. Sci. U S A* **110**,1273-8.

42- Kotiguda G, Weinberg D, Dessau M, Salvi C, Serino G, Chamovitz DA & Hirsch JA (2012) The Organization of a CSN5-containing Subcomplex of the COP9 Signalosome. *J.Biol. Chem.* **287**, 42031-42041.

43- Maytal-Kivity V, Piran R, Pick E, Hofmann K & Glickman MH (2002a) COP9 Signalosome components play a role in the mating pheromone response of S. cerevisiae. *EMBO Rep.* **3**, 1215-1221

44- Tomoda K, Kato JY, Tatsumi E, Takahashi T, Matsuo Y & Yoneda-Kato N (2005) The Jab1/COP9 signalosome subcomplex is a downstream mediator of Bcr-Abl kinase activity and facilitates cell cycle progression. *Blood* **105**, 775–783

45- Tanguy G, Drévillon L, Arous N, Hasnain A, Hinzpeter A, Fritsch J, Goossens M & Fanen P (2008) CSN5 binds to misfolded CFTR and promotes its degradation. *Biochim. Biophys. Acta*

1783, 1189–1199

46- Adler AS, Lin M, Horlings H, Nuyten DS, van de Vijver MJ & Chang HY (2006) Genetic regulators of large-scale transcriptional signatures in cancer. *Nat. Genet.* **38**, 421–430

47- Hallstrom TC & Nevins JR (2006) Jab1 is a specificity factor for E2F1-induced apoptosis. *Genes Dev.* **20**, 613–623

48- Richardson KS & Zundel W (2005) The emerging role of the COP9 signalosome in cancer. *Mol. Cancer Res*. **3**, 645–653

49- Tomoda K, Kato JY, Tatsumi E, Takahashi T, Matsuo Y & Yoneda-Kato N (2004) Multiple functions of Jab1 are required for early embryonic development and growth potential in mice. *J. Biol. Chem.* **279**, 43013–43018

50- Panattoni M, Sanvito F, Basso V, Doglioni C, Casorati G, Montini E, Bender JR, Mondino A, & Pardi R (2008) Targeted inactivation of the COP9 signalosome impairs multiple stages of T cell development. *J. Exp. Med*. **205**, 465–477

51- Suh GS, Poeck B, Chouard T, Oron E, Segal D, Chamovitz DA & Zipursky SL (2002) Drosophila JAB1/CSN5 acts in photoreceptor cells to induce glial cells. *Neuron* **33**, 35–46.

52- Peth A, Berndt C, Henke W & Dubiel W (2007) Downregulation of COP9 signalosome subunits differentially affects the CSN complex and target protein stability. *BMC biochemistry* **8**, 27.

53- Gusmaroli G, Figueroa P, Serino G & Deng XW (2007) Role of the MPN subunits in COP9 signalosome assembly and activity, and their regulatory interaction with Arabidopsis Cullin3-based E3 ligases. *Plant Cell* **19**, 564–581.

54- Gusmaroli G, Feng S & Deng XW (2004) The Arabidopsis CSN5A and CSN5B subunits are present in distinct COP9 signalosome complexes, and mutations in their JAMM domains exhibit differential dominant negative effects on development. *The Plant Cell Online* **16**, 2984.

55- Busch S, Schwier EU, Nahlik K, Bayram O, Helmstaedt K, Draht OW, Krappmann S, Valerius O, Lipscomb WN & Braus GH (2007) An eight-subunit COP9 signalosome with an intact JAMM motif is required for fungal fruit body formation. *Proc Natl Acad Sci USA* **104**, 8089–8094.

56- Busch S, Eckert SE, Krappmann S & Braus GH (2003) The COP9 signalosome is an essential regulator of development in the filamentous fungus Aspergillus nidulans. *Molecular*

microbiology **49**, 717–730.

57- Oron E, Tuller T, Li L, Rozovsky N, Yekutieli D, Rencus-Lazar S, Segal D, Chor B, Edgar BA & Chamovitz DA (2007) Genomic analysis of COP9 signalosome function in Drosophila melanogaster reveals a role in temporal regulation of gene expression. *Mol. Syst. Biol.* **3**, 108.

58- Mundt KE, Liu C, & Carr AM (2002) Deletion mutants in COP9/signalosome subunits in fission yeast Schizosaccharomyces pombe display distinct phenotypes. *Mol Biol Cell* **13**, 493–502.

59- Wang X, Kang D, Feng S, Serino G, Schwechheimer C, & Wei N (2002) CSN1 N-terminal-dependent activity is required for Arabidopsis development but not for Rub1/Nedd8 deconjugation of cullins: a structure-function study of CSN1 subunit of COP9 signalosome. *Mol Biol Cell* **13**, 646–655

60- Wang X, Feng S, Nakayama N, Crosby WL, Irish V, Deng XW & Wei N (2003) The COP9 signalosome interacts with SCF(UFO) and participates in Arabidopsis flower development. *Plant Cell* **15**, 1071–1082

61- Pearce C, Hayden RE, Bunce CM, & Khanim FL (2009) Analysis of the role of COP9 Signalosome (CSN) subunits in K562; the first link between CSN and autophagy. *BMC Cell Biol.* **28**, 10-31

62- Su H, Li F, Ranek MJ, Wei N, & Wang, X (2011) COP9 signalosome regulates autophagosome maturation. *Circulation* **124**, 2117-28.

63- Su H, Li J, Osinska H, Li F, Robbins J, Liu J, Wei N & Wang X (2013) The COP9 Signalosome Is Required for Autophagy, Proteasome-Mediated Proteolysis, and Cardiomyocyte Survival in Adult Mice. *Circ Heart Fail.* **6**, 1049-57.

64- Collins GA & Tansey WP (2006) The proteasome: a utility tool for transcription? *Curr. Opin. Genet. Dev.* **16**, 197-202.

65- O' Connell BC & Harper JW (2007) Ubiquitin proteasome system (UPS): whan can chromatin do for you? *Curr. Opin. Cell. Biol.* **19**, 206-214.

66- Muratani M & Tansey WP (2003) How the ubiquitin-proteasome system controls transcription. *Nat Rev Mol Cell Biol.* **4**, 192-20.

67- Wei N & Deng XW (1992) COP9: a new genetic locus involved in light-regulated development and gene expression in Arabidopsis. *Plant Cell* **4**, 1507–1518

68- Serino G & Deng XW (2003) The COP9 signalosome: regulating plant development through control of proteolysis. *Annu Rev Plant Biol* **54**, 165–182

69- Dohmann EM, Levesque MP, Isono E, Schmid M & Schwechheimer C. (2008) Auxin responses in mutants of the Arabidopsis CONSTITUTIVE PHOTOMORPHOGENIC9 signalosome. *Plant Physiol*. **147**,1369-79

70- Feng S, Ma L, Wang X, Xie D, Dinesh-Kumar SP, Wei N & Deng XW (2003) The COP9 signalosome interacts physically with SCF COI1 and modulates jasmonate responses. *Plant Cell*. **15**,1083-94.

71- Dohmann EM, Levesque MP, De Veylder L, Reichardt I, Jürgens G, Schmid M, & Schwechheimer C (2008) The Arabidopsis COP9 signalosome is essential for G2 phase progression and genomic stability. *Development.* **135**, 2013-22.

72- Menon S, Chi H, Zhang H, Deng XW, Flavell RA, & Wei N. (2007) COP9 signalosome subunit 8 is essential for peripheral T cell homeostasis and antigen receptor-induced entry into the cell cycle from quiescence. *Nat Immunol* **8**, 1236–1245

73- Nahlik K, Dumkow M, Bayram O, Helmstaedt K, Busch S, Valerius O, Gerke J, Hoppert M, Schwier E, Opitz L, Westermann M, Grond S, Feussner K, Goebel C, Kaever A, Meinicke P, Feussner I, & Braus GH (2010) The COP9 signalosome mediates transcriptional and metabolic response to hormones, oxidative stress protection and cell wall rearrangement during fungal development. *Mol Microbiol.* **78**, 964-979

74- Groisman R, Polanowska J, Kuraoka I, Sawada J, Saijo M, Drapkin R, Kisselev AF, Tanaka K, & Nakatani Y. (2003) The ubiquitin ligase activity in the DDB2 and CSA complexes is differentially regulated by the COP9 signalosome in response to DNA damage. *Cell.* **113**, 357-67.

75- Ullah Z, Buckley MS, Arnosti DN & Henry RW (2007) Retinoblastoma protein regulation by the Cop9 signalosome. *Mol Biol Cell* **18**, 1179-1186.

76- Mundt KE, Porte J, Murray JM, Brikos C, Chrinstensen PU, Caspari T, Hagan IM, Millar JBA, Simanis V, Hofmaan K & Carr AM (1999) The COP9/signalosome complex is conserved in

fission yeast and has a role in S phase. *Curr Biol* **9**, 1427–1430.

77- He Q, Cheng P, He Q, & Liu Y (2005). The COP9 signalosome regulates the Neurospora circadian clock by controlling the stability of the SCFFWD-1 complex. *Genes Dev* **19**, 1518–1531.

78- Rosel D & Kimmel AR (2006) The COP9 signalosome regulates cell proliferation of Dictyostelium discoideum. *Eur J Cell Biol* **85**, 1023–1034.

79- Braus GH, Irniger S & Bayram O (2010) Fungal development and the COP9 signalosome. *Curr Opin Microbiol.* **13**, 672-676.

80- Wee S, Hetfeld B, Dubiel W & Wolf DA. (2002) Conservation of the COP9/signalosome in budding yeast. *Bmc Genet.* **3**, 15

81- Yu Z, Kleifeld O, Lande-Atir A, Bsoul M, Kleiman M, Krutauz D, Book A, Vierstra RD, Hofmann K, Reis N, Glickman MH & Pick, E. (2011) Dual function of Rpn5 in two PCI complexes, the 26S proteasome and COP9 signalosome. *Mol. Biol. Cell* **22**, 911–920.

82- Bosu DR & Kipreos ET (2008) Cullin-RING ubiquitin ligases: global regulation and activation cycles. *Cell Div.* **3**, 7.

83- Maytal-Kivity V, Pick E, Piran R, Hofmann K & Glickman MH. (2003) The COP9 signalosome-like complex in S. cerevisiae and links to other PCI complexes. *Int. J. Biochem. Cell Biol.* **35**, 706–715.

84- Pick E, Golan A, Zimbler JZ, Guo L, Sharaby Y, Tsuge T, Hofmann K & Wei N. (2012) The minimal deneddylase core of the COP9 signalosome excludes the Csn6 MPN- domain. *Plos One* **7**, e43980.

85- Zemla A, Thomas Y, Kedziora S, Knebel A, Wood NT, Rabut G & Kurz T (2013) CSN- and CAND1-dependent remodelling of the budding yeast SCF complex. *Nat. Commun*. **4**, 1641

86- Boorsma A, Foat BC, Vis D, Klis F & Bussemaker HJ (2005) T-profiler: scoring the activity of predefined groups of genes using gene expression data. *Nucleic Acids Res.* **33**, W592–595.

87- Harbison CT, Gordon DB, Lee TI, Rinaldi NJ, Macisaac KD, Danford TW, Hannett NM, Tagne J-B, Reynolds DB, Yoo J, Jennings EG, Zeitlinger J, Pokholok DK, Kellis M, Rolfe PA, Takusagawa KT, Lander ES, Gifford DK, Fraenkel E & Young RA (2004) Transcriptional regulatory code of a eukaryotic genome. *Nature* **431**, 99–104.

88- Pfeifer K, Kim KS, Kogan S & Guarente L (1989) Functional dissection and sequence of yeast HAP1 activator. *Cell* **56**, 291–301.

89- Smith SA, Kumar P, Johnston I & Rosamond J (1992) SCM4, a gene that suppresses mutant cdc4 function in budding yeast. *Mol. Gen. Genet.* **235**, 285–291.

90- Eide DJ. (2009) Homeostatic and adaptive responses to zinc deficiency in Saccharomyces cerevisiae. *J. Biol. Chem.* **284**, 18565–18569.

91- Mukhopadhyay K, Prasad T, Saini P, Pucadyil TJ, Chattopadhyay A & Prasad R. (2004) Membrane sphingolipid-ergosterol interactions are important determinants of multidrug resistance in Candida albicans. Antimicrob. *Agents Chemother.* **48**, 1778–1787.

92- Pfaller MA, Riley J & Koerner T (1990) Effects of terconazole and other azole antifungal agents on the sterol and carbohydrate composition of Candida albicans. *Diagn. Microbiol. Infect. Dis.* **13**, 31-35.

93- Sanati H, Belanger P, Fratti R & Ghannoum M (1997) A new triazole, voriconazole (UK-109,496), blocks sterol biosynthesis in Candida albicans and Candida krusei. *Antimicrobial Agents and Chemotherapy* **41**, 2492-2496.

94- Welihinda AA, Beavis AD & Trumbly RJ (1994) Mutations in LIS1 (ERG6) gene confer increased sodium and lithium uptake in Saccharomyces cerevisiae. *Biochim. Biophys. Acta* **1193**, 107–117.

95- Loukin SH, Kung C & Saimi Y (2007) Lipid perturbations sensitize osmotic down-shock activated Ca2+ influx, a yeast "deletome" analysis. *Faseb J. Off. Publ. Fed. Am. Soc. Exp. Biol.* **21**, 1813–1820.

96- Yuan DS (2011) Dithizone staining of intracellular zinc: an unexpected and versatile counterscreen for auxotrophic marker genes in Saccharomyces cerevisiae. *Plos One* **6**, e25830.

97- Ezaki B & Nakakihara E (2012) Possible involvement of GDI1 protein, a GDP dissociation inhibitor related to vesicle transport, in an amelioration of zinc toxicity in Saccharomyces cerevisiae. *Yeast Chichester Engl.* **29**, 17–24.

98- Ma L, Zhao H & Deng XW (2003) Analysis of the mutational effects of the COP/DET/FUS loci on genome expression profiles reveals their overlapping yet not identical roles in regulating Arabidopsis seedling development. *Dev. Camb. Engl.* **130**, 969–981.

99- Xirodimas DP, Sundqvist A, Nakamura A, Shen L, Botting C & Hay RT (2008) Ribosomal proteins are targets for the NEDD8 pathway. *EMBO Rep.* **9**, 280–286.

100- Costanzo M, Baryshnikova A, Bellay J, Kim Y, Spear ED, Sevier CS, Ding H, Koh JLY, Toufighi K, Mostafavi S, Prinz J, St Onge RP, VanderSluis B, Makhnevych T, Vizeacoumar FJ, Alizadeh S, Bahr S, Brost RL, Chen Y, Cokol M, Deshpande R, Li Z, Lin Z-Y, Liang W, Marback M, Paw J, San Luis B-J, Shuteriqi E, Tong AHY, van Dyk N, Wallace IM, Whitney JA, Weirauch MT, Zhong G, Zhu H, Houry WA, Brudno M, Ragibizadeh S, Papp B, Pál C, Roth FP, Giaever G, Nislow C, Troyanskaya OG, Bussey H, Bader GD, Gingras A-C, Morris QD, Kim PM, Kaiser CA, Myers CL, Andrews BJ & Boone C (2010) The genetic landscape of a cell. *Science* **327**, 425–431.

101- Chen F, Zhou J, Shi Z, Liu L, Du G & Chen J (2010) [Effect of acetyl-CoA synthase gene overexpression on physiological function of Saccharomyces cerevisiae]. *Wei Sheng Wu Xue Bao* **50**, 1172–1179.

102- Galdieri L & Vancura A (2012) Acetyl-CoA carboxylase regulates global histone acetylation. *J. Biol. Chem.* **287**, 23865–23876.

103- Nielsen J (2009) Systems biology of lipid metabolism: from yeast to human. *FEBS Lett.* **583**, 3905–3913.

104- Fowler DM, Cooper SJ, Stephany JJ, Hendon N, Nelson S & Fields S (2011) Suppression of statin effectiveness by copper and zinc in yeast and human cells. *Mol. Biosyst.* **7**, 533–544.

105- Uttenweiler A, Schwarz H, Neumann H & Mayer A (2007) The vacuolar transporter chaperone (VTC) complex is required for microautophagy. *Mol. Biol. Cell* **18**, 166–175.

106- Pagani MA, Casamayor A, Serrano R, Atrian S & Ariño J (2007) Disruption of iron homeostasis in Saccharomyces cerevisiae by high zinc levels: a genome-wide study. *Mol. Microbiol.* **65**, 521–537.

107- Wu C-Y, Roje S, Sandoval FJ, Bird AJ, Winge DR & Eide DJ (2009) Repression of sulfate assimilation is an adaptive response of yeast to the oxidative stress of zinc deficiency. *J. Biol. Chem.* **284**, 27544–27556.

108- Eide D & Guarente L (1992) Increased dosage of a transcriptional activator gene enhances iron-limited growth of Saccharomyces cerevisiae. *J. Gen. Microbiol.* **138**, 347–354

109- Yuan DS (2011) Dithizone staining of intracellular zinc: an unexpected and versatile counterscreen for auxotrophic marker genes in Saccharomyces cerevisiae. *PloS One* **6**, e25830.

110- Lemoine S, Combes F, Servant N & Crom SL (2006) Goulphar: rapid access and expertise for standard two-color microarray normalization methods. *BMC Bioinformatics.* **7**, 467.

111- Edgar R, Domrachev M & Lash AE (2002) Gene Expression Omnibus: NCBI gene expression and hybridization array data repository. *Nucleic Acids Res.* **30**, 207–210.

112- Livak KJ & Schmittgen TD (2001) Analysis of relative gene expression data using real-time quantitative PCR and the 2(-Delta Delta C(T)) *Method. Methods San Diego Calif* **25**, 402–408.

113- Wiśniewski JR, Zougman A, Nagaraj N & Mann M (2009) Universal sample preparation method for proteome analysis. *Nat. Methods* **6**, 359–362.

114- Cox J & Mann M (2008) MaxQuant enables high peptide identification rates, individualized p.p.b.-range mass accuracies and proteome-wide protein quantification. *Nat. Biotechnol.* **26**, 1367–1372.

115- Cox J, Neuhauser N, Michalski A, Scheltema RA, Olsen JV & Mann M (2011) Andromeda: a peptide search engine integrated into the MaxQuant environment. *J. Proteome Res.* **10**, 1794–1805.

116- Gachotte D, Eckstein J, Barbuch R, Hughes T, Roberts C & Bard M (2001) A novel gene conserved from yeast to humans is involved in sterol biosynthesis. *J. Lipid Res*. **42**, 150–154.

MY PAPER INCLUDED IN THE THESIS

- **Salvi C**, Licursi V, De Cesare V, Rinaldi T, Mattei B, Fabbri C, Serino G, Zimbler JZ, Pick E, Barnes B, Bard M & Negri R (2013) The Cop9 signalosome is involved in the regulation of lipid metabolism and of transition metals uptake in *S.cerevisiae. FEBS J.* doi: 10.1111

MY PAPER NOT RELEVANT TO THE THESIS

- Kotiguda GG, Weinberg D, Dessau M, **Salvi C**, Serino G, Chamovitz DA & Hirsch JA (2012) The organization of a CSN5-containing subcomplex of the COP9 signalosome. *J Biol Chem*. **287(50)**, 42031-41.

ACKONLEDGEMENTS

This work was supported by FIRB 2011-2013 (grant no. RBIN06E9Z8) 'Molecular Bases of Diseases', PRIN 2009 'Role of *S. cerevisiae* General Regulatory Factors (GRF) in Chromatin Organization and Dynamics' and Progetti di Ricerca di Ateneo (grant no. C26A1139XY) to Rodolfo Negri; Israel Ministry of Science and Technology (MOST) – Italy Ministry of Foreign Affairs (MAE) grant 3-9022 to Rodolfo Negri, Teresa Rinaldi, Giovanna Serino and Elah Pick; and Israel Science Foundation grant (EP355/10) for Elah Pick; Progetto di Ricerca C26A1089CJ (2010), Sapienza Universita' di Roma, to Rodolfo Negri, Teresa Rinaldi and Giovanna Serino. Valerio Licursi' s fellowship is supported by a grant from Regione Lazio.